2. SRFための超伝導の基礎知識

2.1 Superconductivity
2.2 Thermal conductivity in super-conducting state
2.3 Impurity and RRR
2.4 Surface resistance in AC application
2.5 Critical RF magnetic field in AC application

Basic of Superconductivity and SC Characteristic of Niobium material

- Critical Magnetic Field
- Penetration Depth, Coherence Length, G-L Parameter, RF critical magnetic field
- Thermal Conductivity
- RRR Measurement
- Surface Resistance in AC Application

SRF Specifics and Constrains

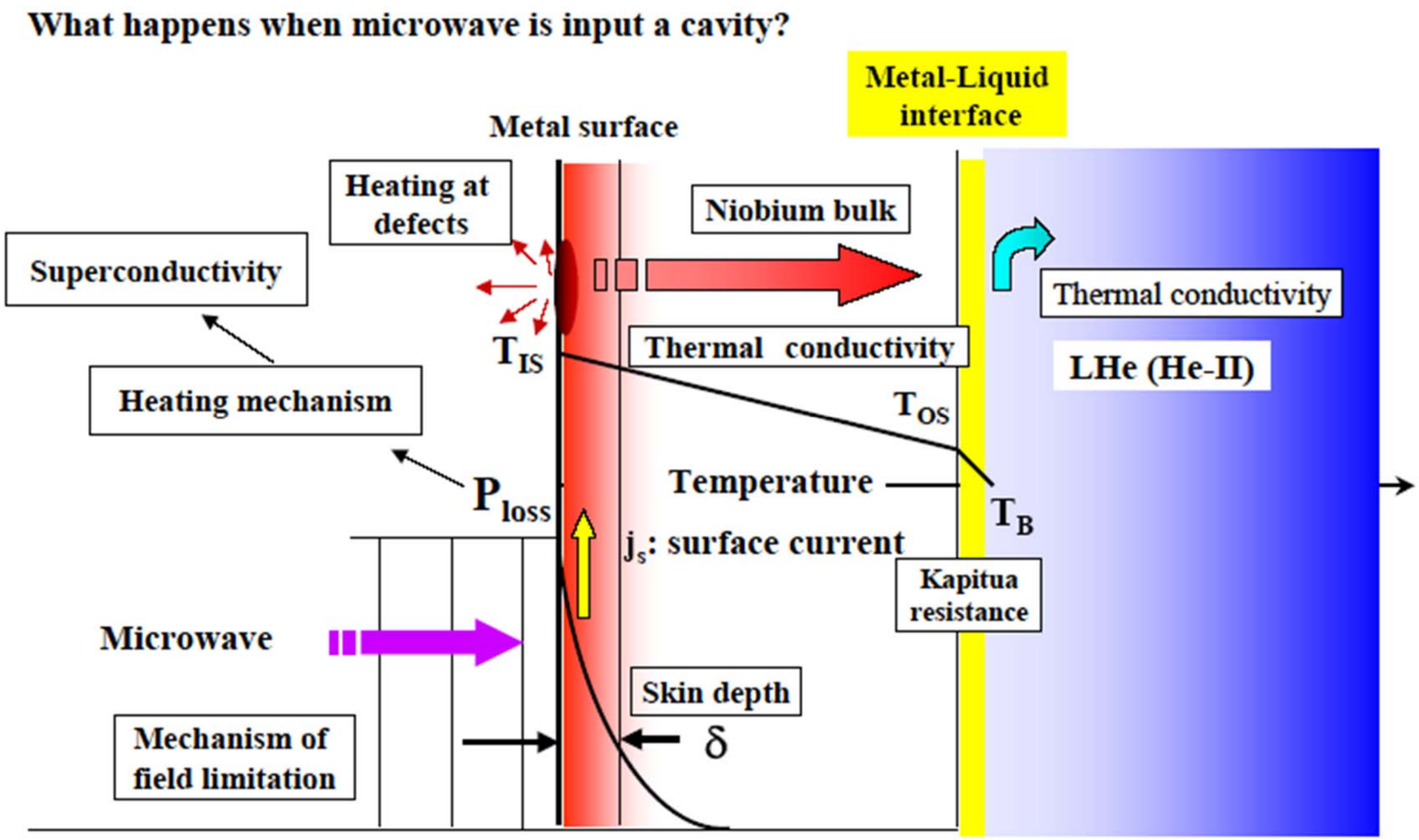

Surface resistance is very very small.

➡ Cavity performance strongly depends on the surface.

Thermal conductivity @ superconducting state is very small.

➡ *High thermal conductivity* is very important.

Superconductivity：現象

1911 by K.Onnes

19933 by Meissner and Ochsenfeld (experiment)
1935 Phenomenological theory by F.and H.London

Zero resistance @ Tc

Perfect diamagnetism < Hc

Miessner effect

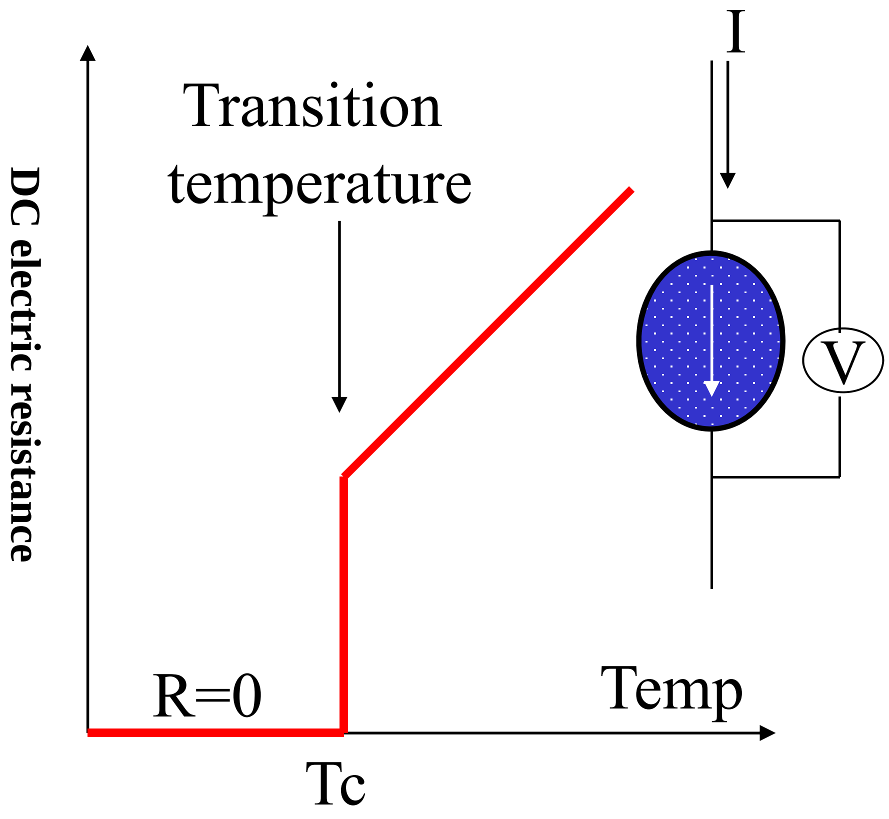

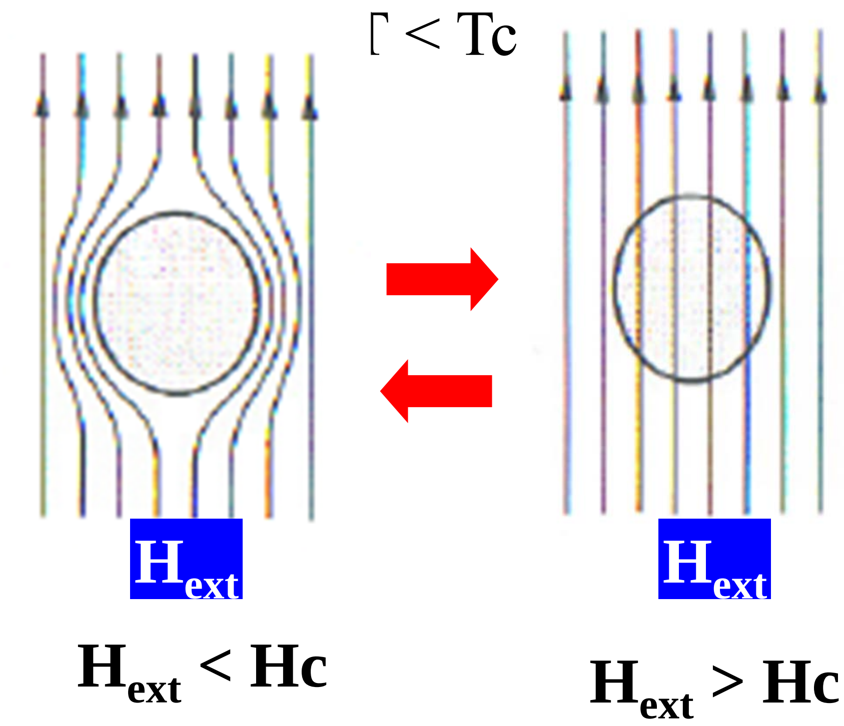

完全導体と超伝導体の相違

慣性法則

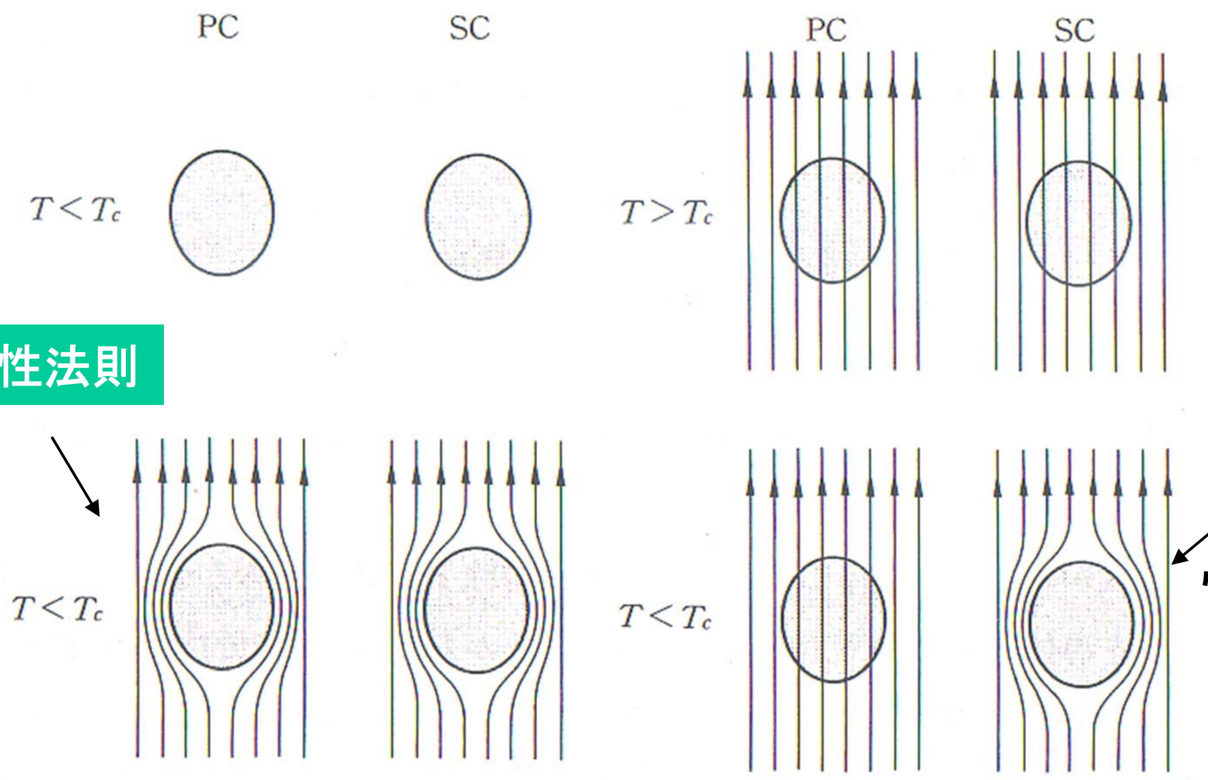

Meissner effect

慣性法則では説明出来ない。
慣性法則は時空の性質。
Meissner効果は、物質特有の性質。

（a） 完全導体，超伝導体になってから（$T<T_c$ の後）磁界が印加された場合

（b） 完全導体，超伝導体になる前（$T>T_c$）に磁界が印加され，後に $T<T_c$ 状態にし，完全導体，超伝導体にした場合

図 3.4 T（温度）$<T_c$（臨界温度）において，完全導体 PC と超伝導体 SC からなる素材の外部磁界に対する相違

Electron-electron interaction through lattice in superconducting state

Electron/electronはクーロン斥力相互作用するが、latticeを介した相互では引力となり得る。 ⟶ 超伝導

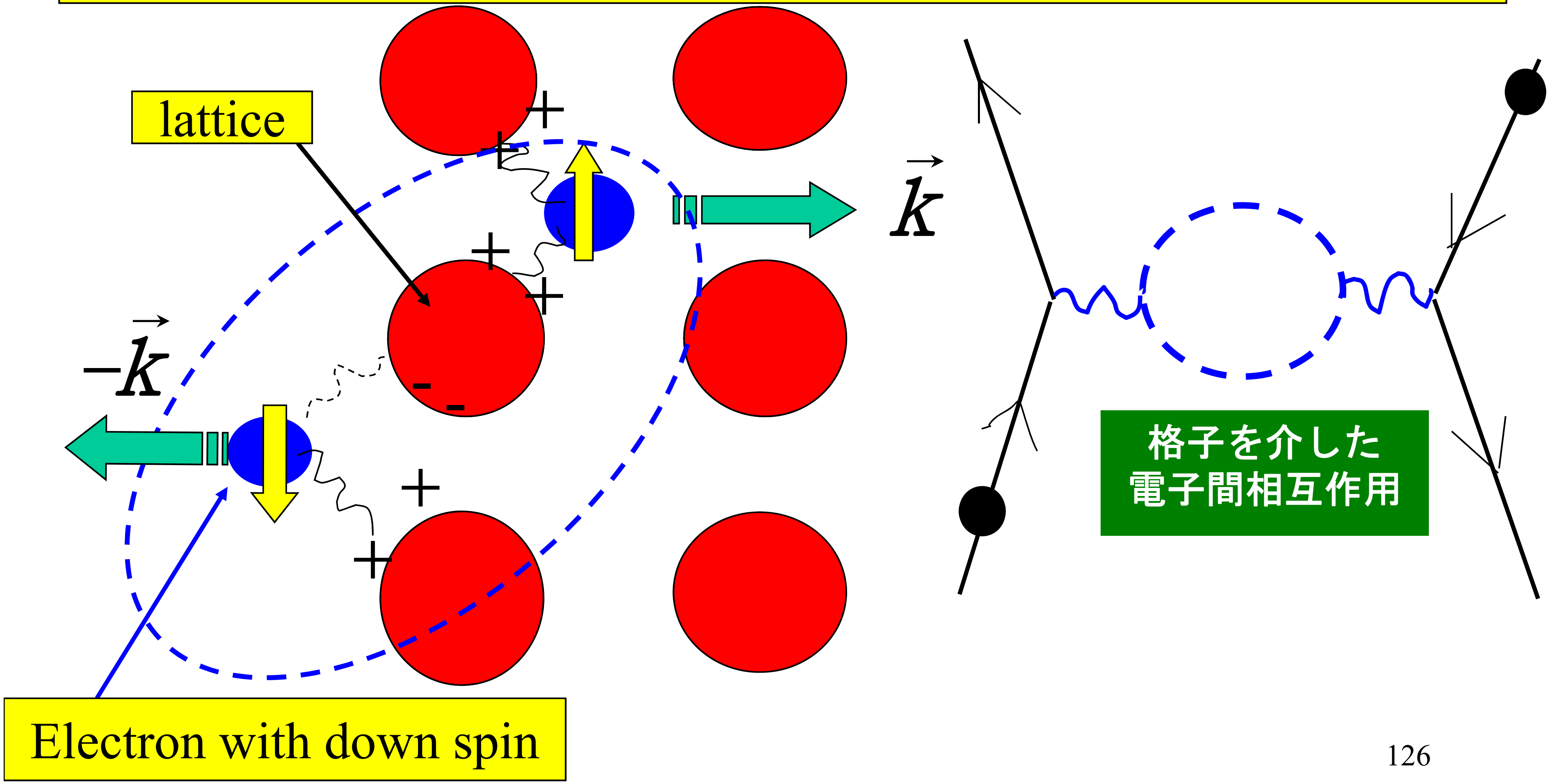

History of Superconductivity

1908 液体ヘリウムの製造、H.K. Onnes
1911 Discovery, H.K Onnes. 永久電流、臨界磁場
（1913 ノーベル物理学賞：液体ヘリウムの製造に至る低温物性の研究）
1933 磁場排除、Meissner and Ochsenfeld
1934 二流体モデル、Gorter and Casimir
1935 現象論的理論(ロンドン侵入長）、F.London and H.London
1937 Type-II超伝導体の発見、Schubnikov
1950 超伝導の現象的理論(GL理論）、Ginzburug and Landau
電子・フォノン相互作用の指摘、Fröhlich
Tcのアイソトープ効果、Maxwell, Reynolds
1953 コヒーレンス長の概念(ロンドン方程式に非局所化）、エネルギーギャップの予言 Pippard
エネルギーギャップの実験的証拠、Goodman and others
1957 BCS理論(超伝導の微視的理論）、Bardeen, Cooper, and Schriefer
（1972 ノーベル物理学賞：超伝導に関するBCS理論）
Type-IIの超伝導理論、Abrikosov
（2003 ノーベル物理学賞：超伝導・超流動の理論に対する先駆的貢献）
1960 超伝導における対象性の自発的破れ、Nambu, Goldstone, Anderson
1961 フラクソイドの量子化の検証、Fairbank, Näbauer
1962 Josenphson効果、 Josephson
1986 高温酸化物超伝導の発見、Bednorz, Müller

Superconductors

Table 1 Superconductivity parameters of the elements

An asterisk denotes an element superconducting only in thin films or under high pressure in a crystal modification not normally stable. Data courtesy of B. T. Matthias, revised by T. Geballe.

Transition temperature in K
Critical magnetic field at absolute zero in gauss (10^{-4} tesla)

Li	Be 0.026											B	C	N	O	F	Ne
Na	Mg											Al 1.140 105	Si*	P*	S*	Cl	Ar
K	Ca	Sc	Ti 0.39 100	V 5.38 1420	Cr*	Mn	Fe	Co	Ni	Cu	Zn 0.875 53	Ga 1.091 51	Ge*	As*	Se*	Br	Kr
Rb	Sr	Y*	Zr 0.546 47	Nb 9.50 1980	Mo 0.92 95	Tc 7.77 1410	Ru 0.51 70	Rh .0003 .049	Pd	Ag	Cd 0.56 30	In 3.4035 293	Sn (w) 3.722 309	Sb*	Te*	I	Xe
Cs*	Ba*	La fcc 6.00 1100	Hf 0.12	Ta 4.483 830	W 0.012 1.07	Re 1.4 198	Os 0.655 65	Ir 0.14 19	Pt	Au	Hg (α) 4.153 412	Tl 2.39 171	Pb 7.193 803	Bi*	Po	At	Rn
Fr	Ra	Ac															

Ce*	Pr	Nd	Pm	Sm	Eu	Gd	Tb	Dy	Ho	Er	Tm	Yb	Lu 0.1
Th 1.368 1.62	Pa 1.4	U*(α)	Np	Pu	Am	Cm	Bk	Cf	Es	Fm	Md	No	Lr

Critical magnetic field measurement

$$V = V_A + V_B = -\frac{d}{dt}\Phi_A + \frac{d}{dt}\Phi_B$$

$$(-nS_0\mu\frac{d}{dt}B_{ext} + \frac{d}{dt}M) + nS_0\mu\frac{d}{dt}B_{ext}$$

$$= \frac{d}{dt}M$$

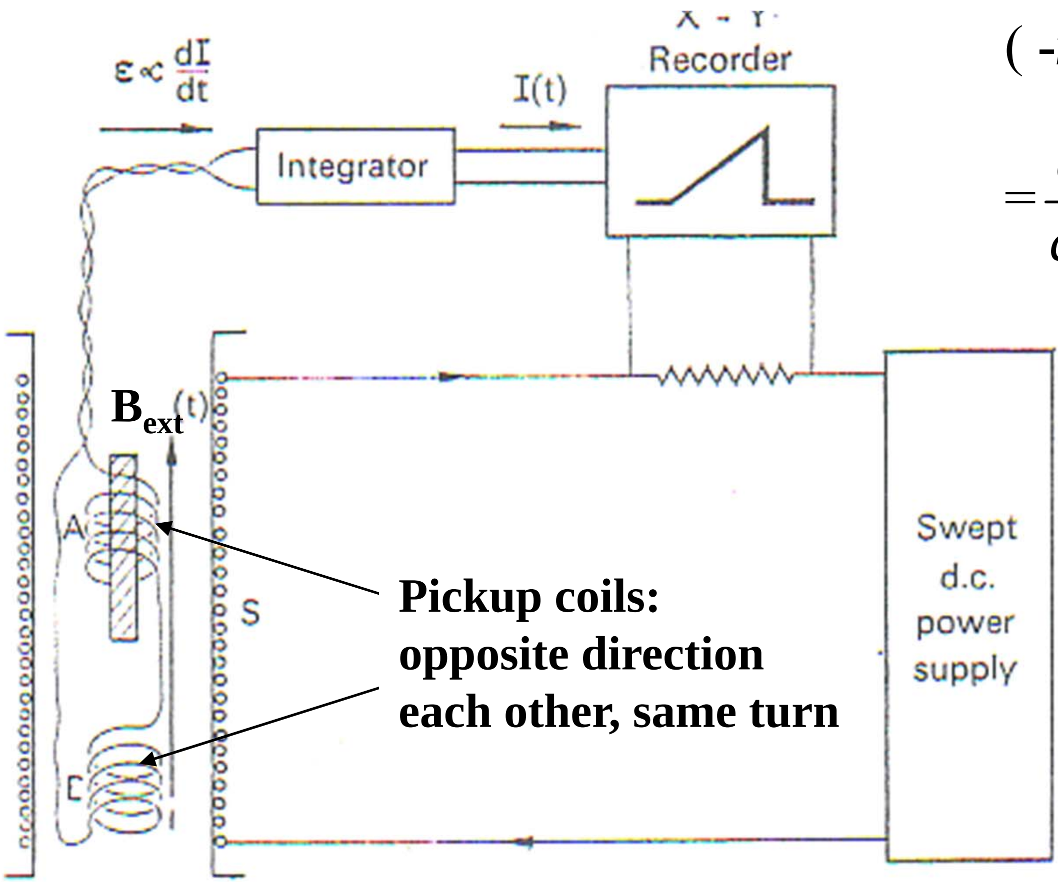

$$M = \int_0^t V dt$$

Two types of superconductor

Type-I

$$\frac{\lambda}{\xi} \le \frac{1}{\sqrt{2}}$$

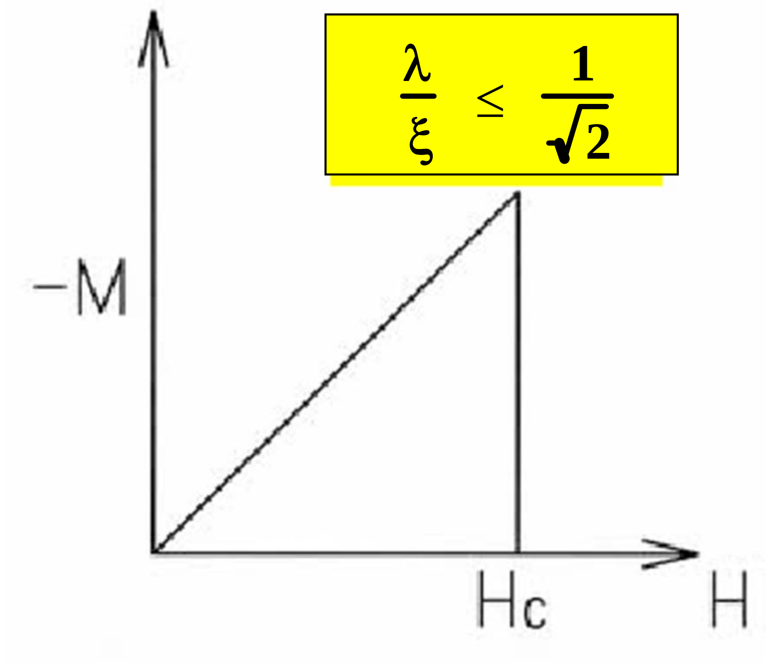

Type-II

$$\frac{\lambda}{\xi} > \frac{1}{\sqrt{2}}$$

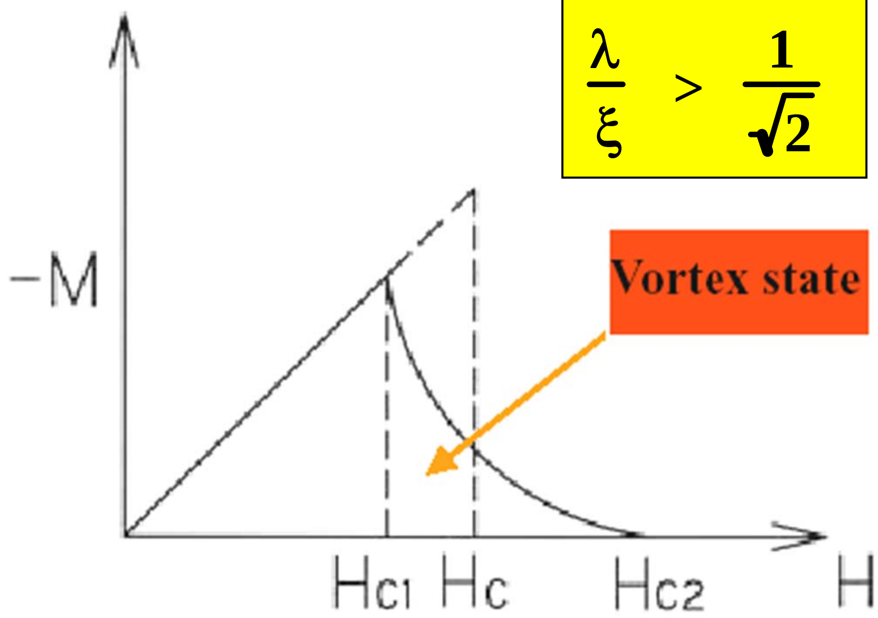

Vortex state

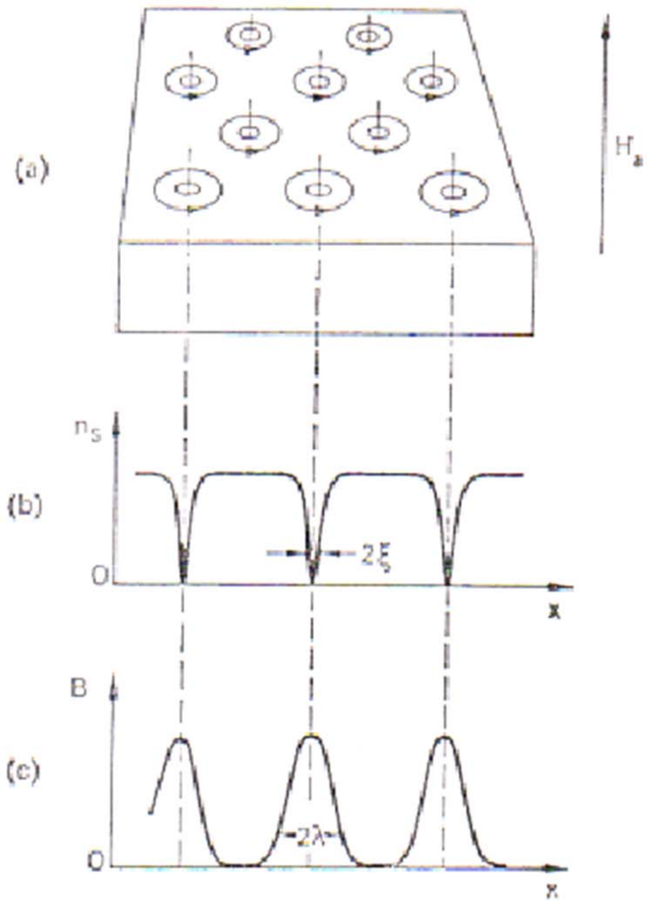

Vortex state

ξ : Coherence length
size of Cooper pair

鉄粉を付けて観察

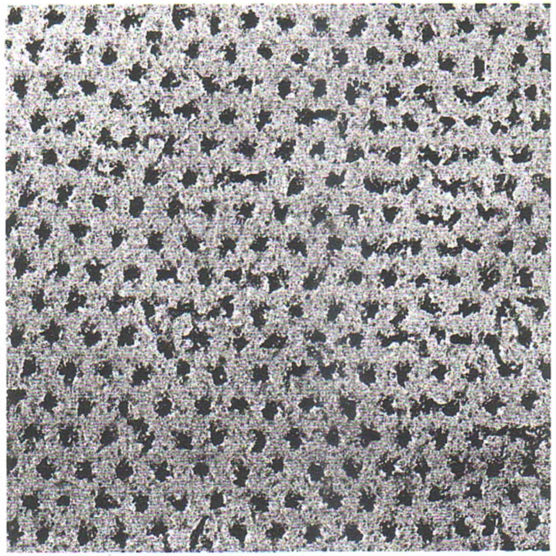

Figure 19 Triangular lattice of fluxoids through top surface of a superconducting cylinder. The points of exit of the flux lines are decorated with fine ferromagnetic particles. The electron microscope image is at a magnification of 8300, by U. Essmann and H. Träuble.

λ_L : London penetration depth

Depth of penetration of the magnetic field

Electron Phorographyによるvortexの観察

By A.Tonomura et al.

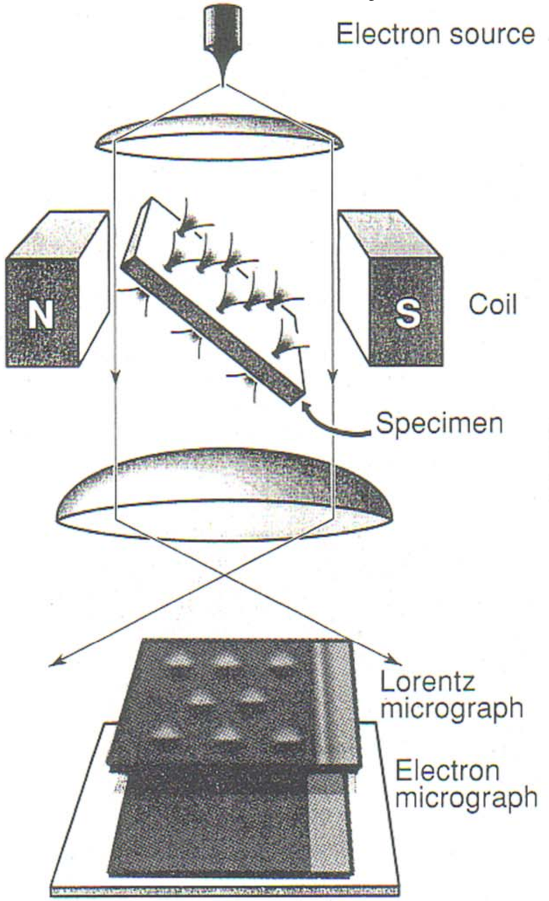

FIG. 1 Schematic diagram of vortex-lattice observation.

６本の量子fluxの束が観測されている。

Miessner state

Vortex state

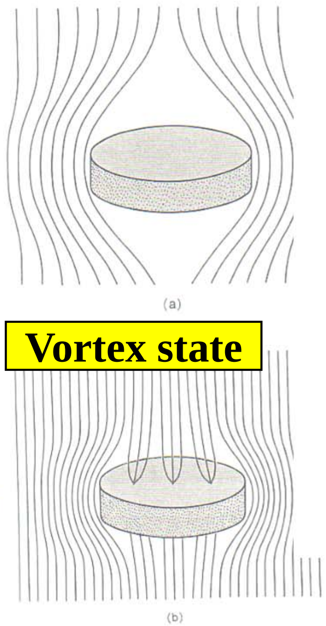

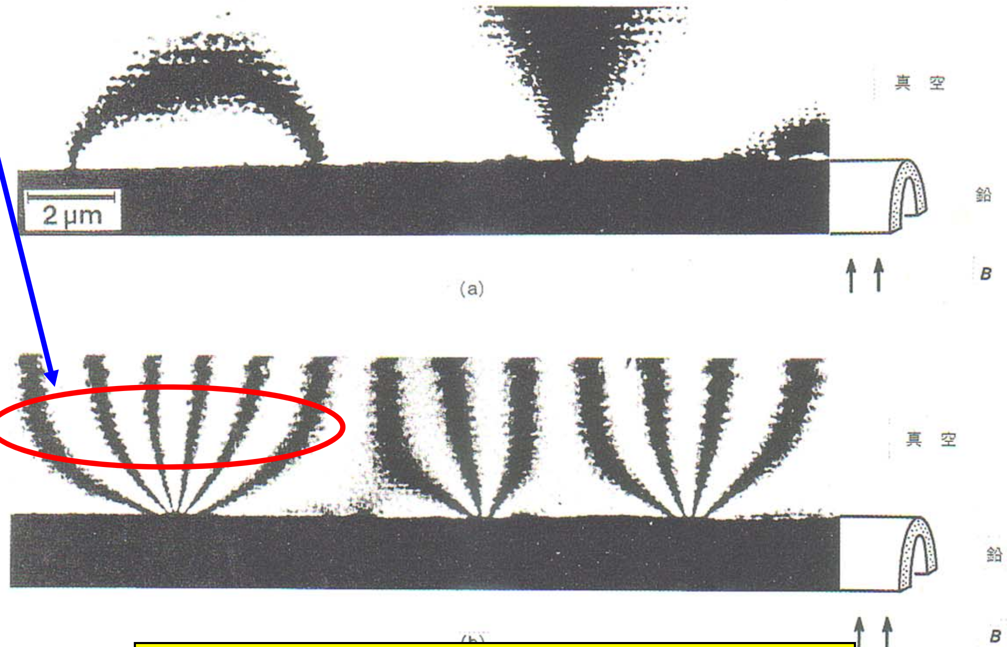

鉛のvortex 観察

Vortex on Nb film

Vortex lattice on Nb film

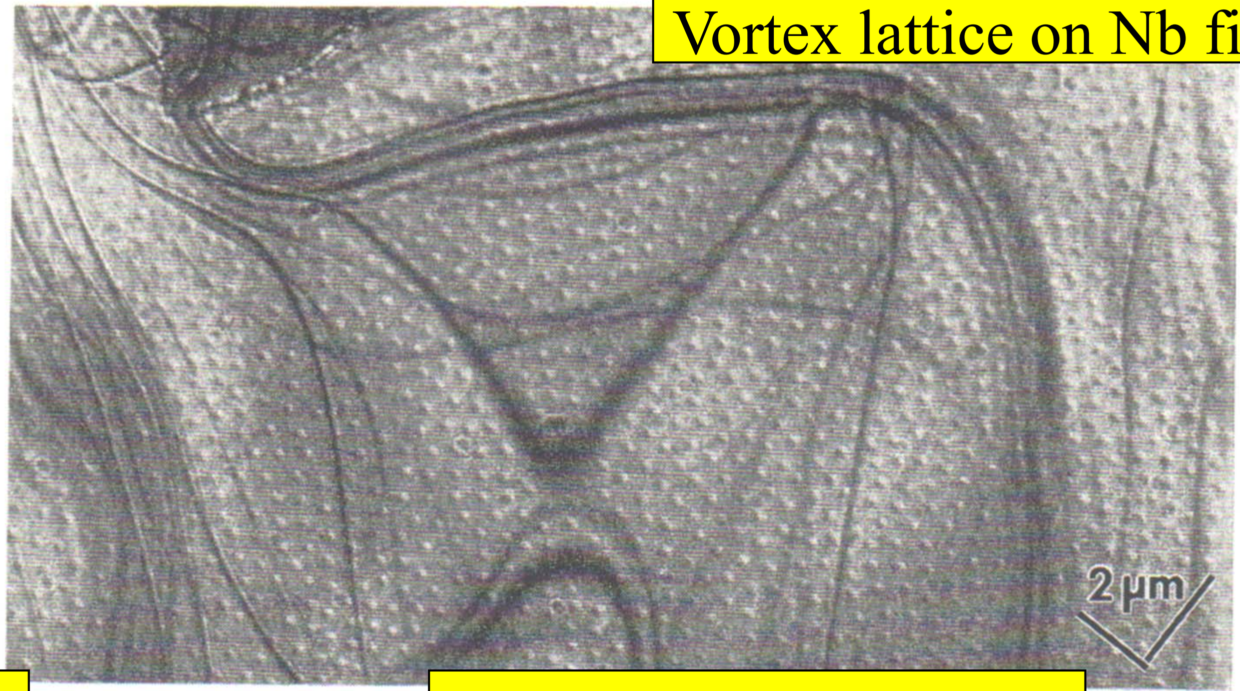

FIG. 2 Lorentz micrograph of a Nb thin film. A magnetic field of 100 G is applied to the film in the superconducting state at 4.5 K. Vortices are observed as small globules, each with black and white contrast. The magnification differs in the two directions by $\sqrt{2}$, because the film is tilted by 45°. The dark lines are bend contours.

T-dependence of vortex size

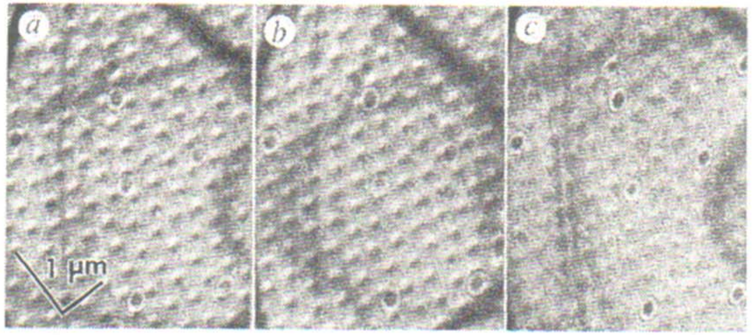

FIG. 3 Dependence of the vortex images on temperature. *a*, $T=4.5$ K; *b*, $T=6.0$ K; *c*, $T=8.0$ K. The vortices become larger as the penetration depth increases with temperature. The vortex configuration, random at 4.5 K, turns into a more and more regular hexagonal lattice at higher *T*, which can be recognized more easily when the photographs are seen obliquely.

Vortex hopping after switched off

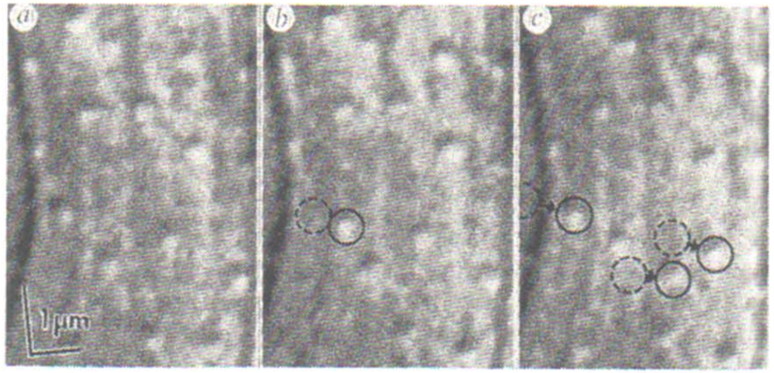

FIG. 4 Dynamics of the vortices as seen at times t after magnetic field has been switched off from 150 G. *a*, $t=t_0+0$ s; *b*, $t=t_0+0.1$ s; *c*, $t=t_0+1.4$ s ($t_0=170$ s). Dotted and solid circles show vortex positions before and after hopping, and the hopping directions are indicated by the arrows.

Abrikosov Theory

Type-I superconductivity

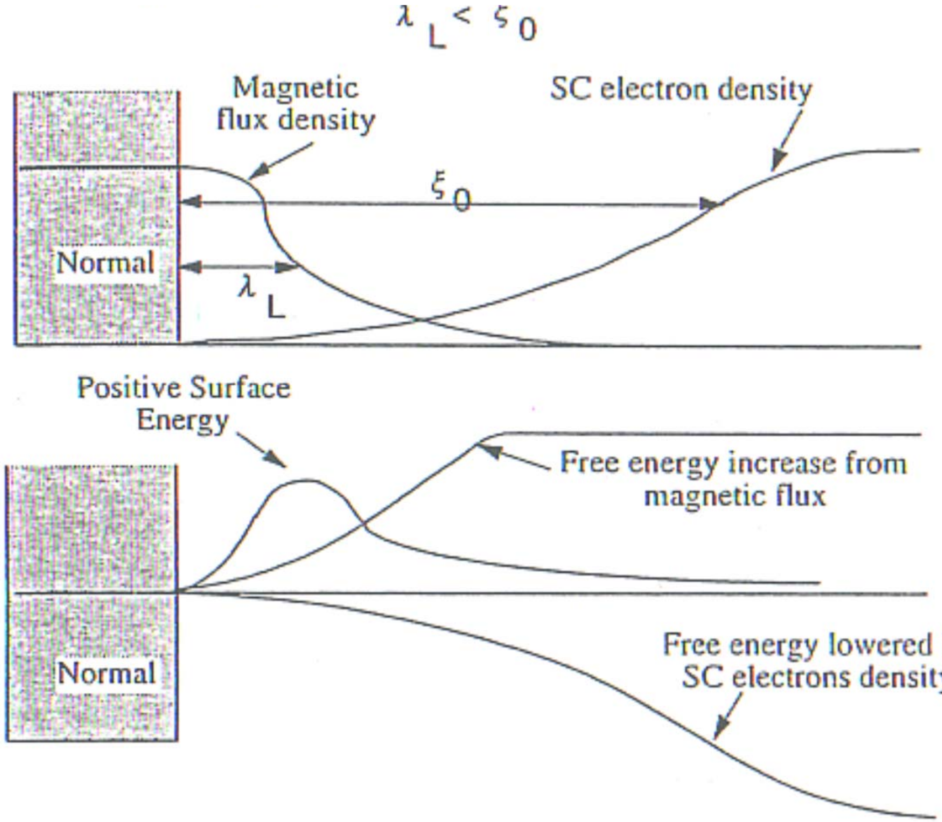

$$\sigma_{ns} \equiv \int_{-\infty}^{\infty} dz \left\{ g_{sH} - g_n \right\}$$

$$\kappa \equiv \frac{\lambda}{\xi} = \frac{\sqrt{2} e^*}{\hbar c} H_c \lambda^2$$

$$\kappa < \frac{1}{\sqrt{2}} \ \textbf{: type - I} \quad (\sigma_{ns} > 0)$$

Abrikosov Theory

Type-II superconductor

$\lambda_L > \xi_0$

$$\kappa > \frac{1}{\sqrt{2}} \ \textbf{: type - II} \ \ (\sigma_{ns} < 0)$$

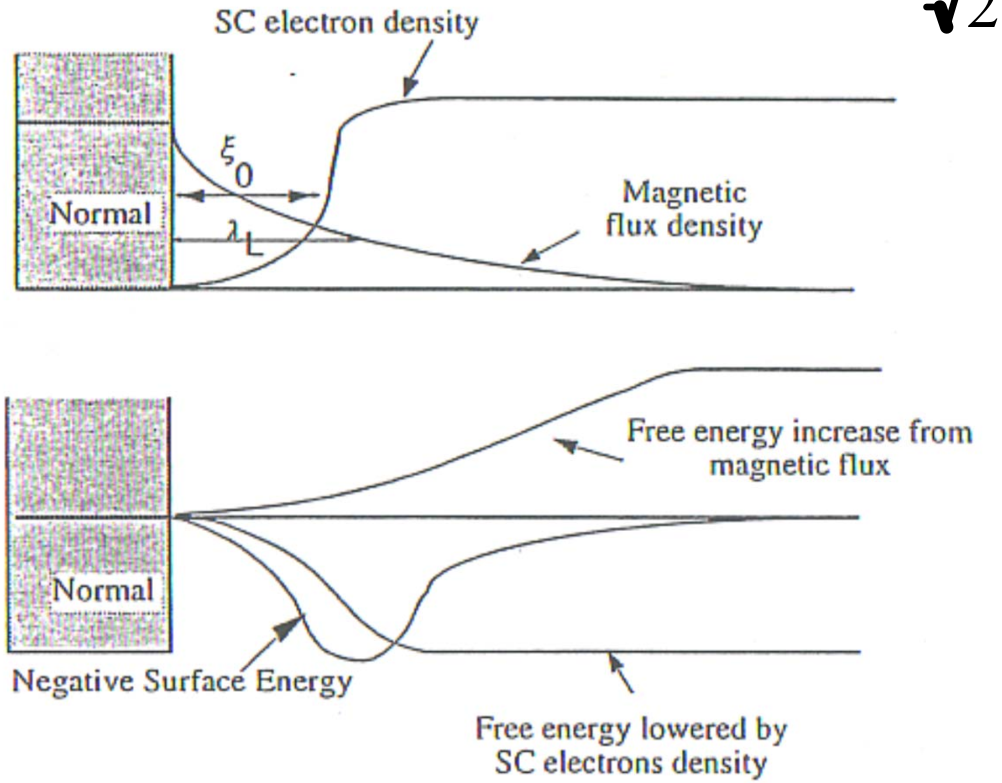

Critical magnetic field measurement

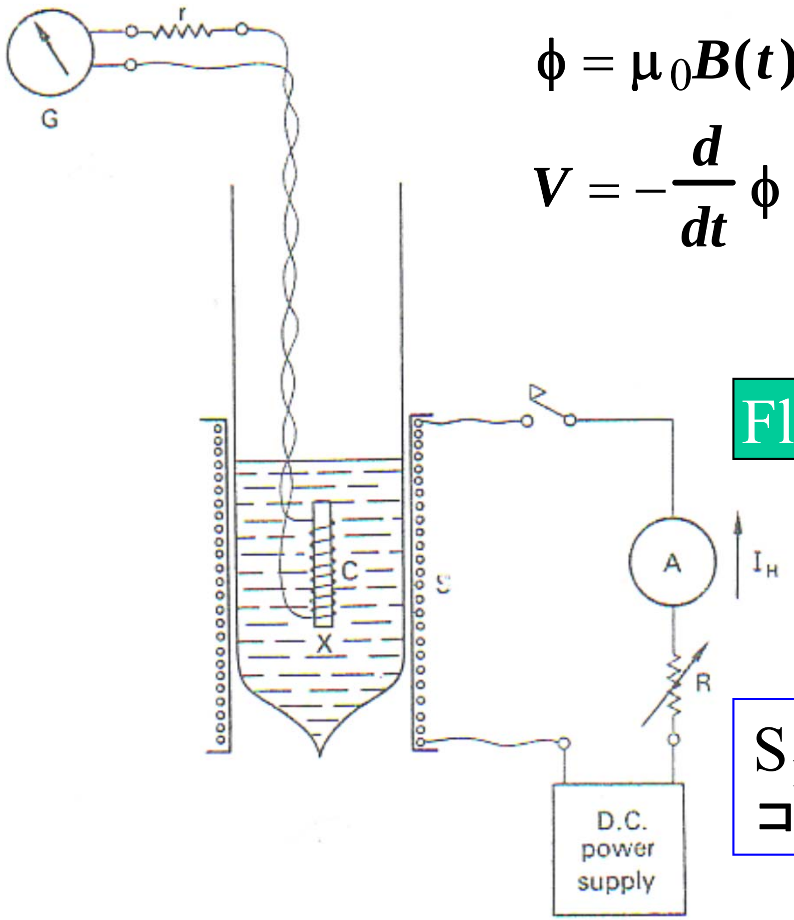

$$\phi = \mu_0 B(t)\cdot[S_1 + S_s(t)],\ B(t) = B_0 t$$

$$V = -\frac{d}{dt}\phi = -\mu_0 B_0 S_1 - \mu_0 B_0 S_s - \mu_0 B_0 t \frac{d}{dt} S_s$$

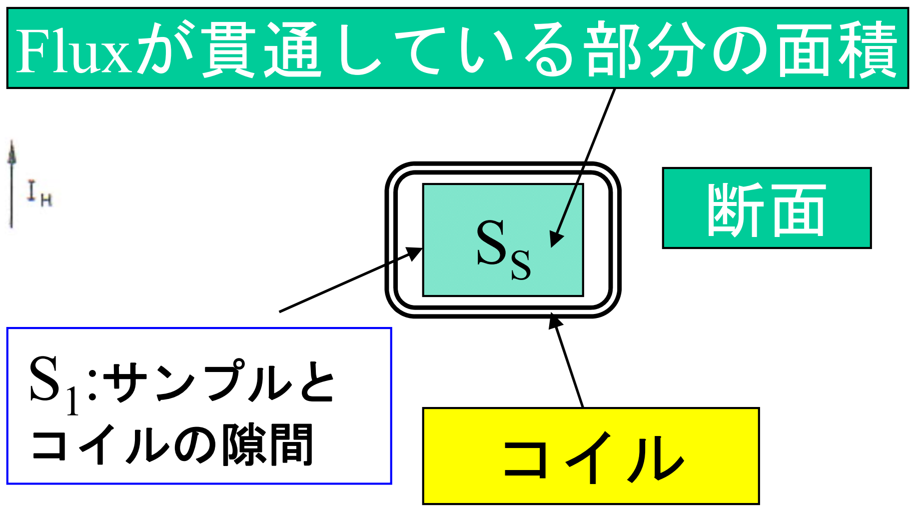

Critical magnetic field measurement - 1

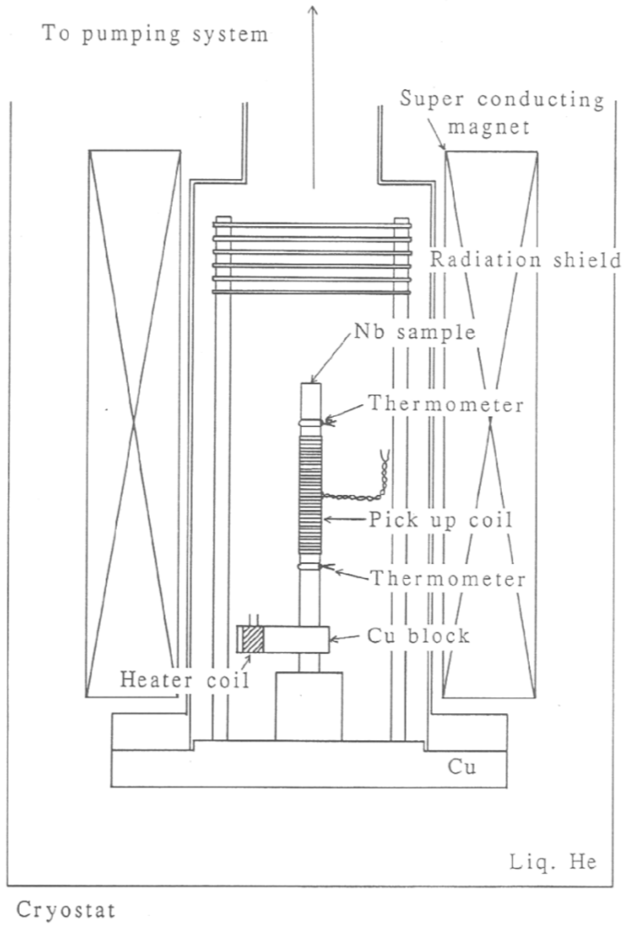

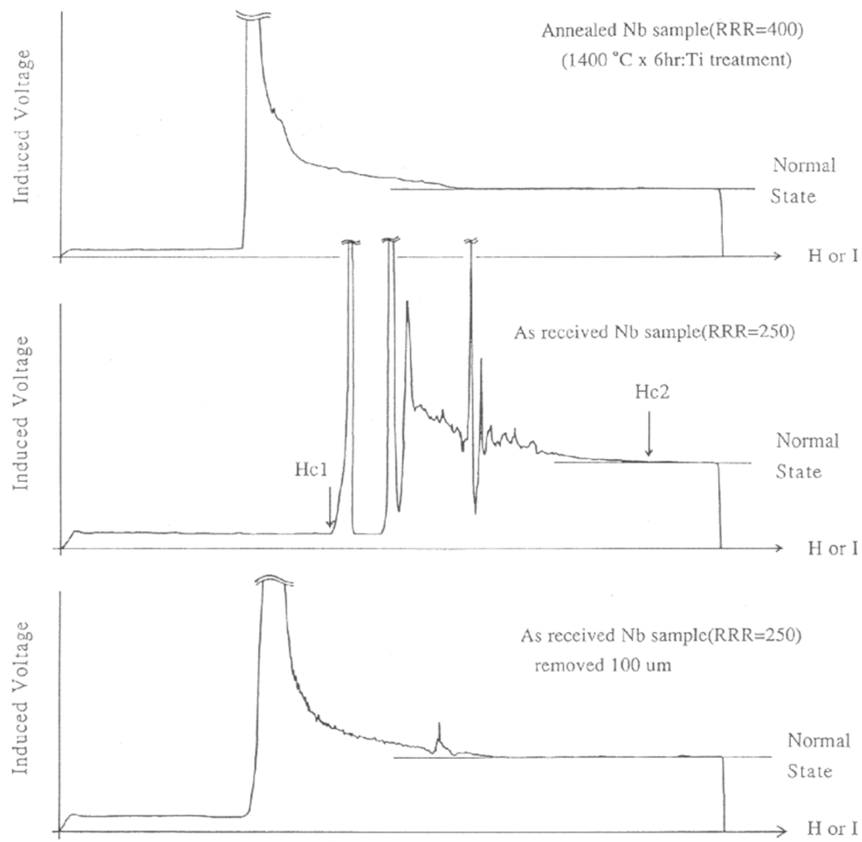

Critical magnetic field measurement - 2

$$V = V_A - V_B \propto \frac{d}{dt}\mu_0(H+M) - \frac{d}{dt}\mu_0 H$$

$$\propto -\frac{d}{dt}M$$

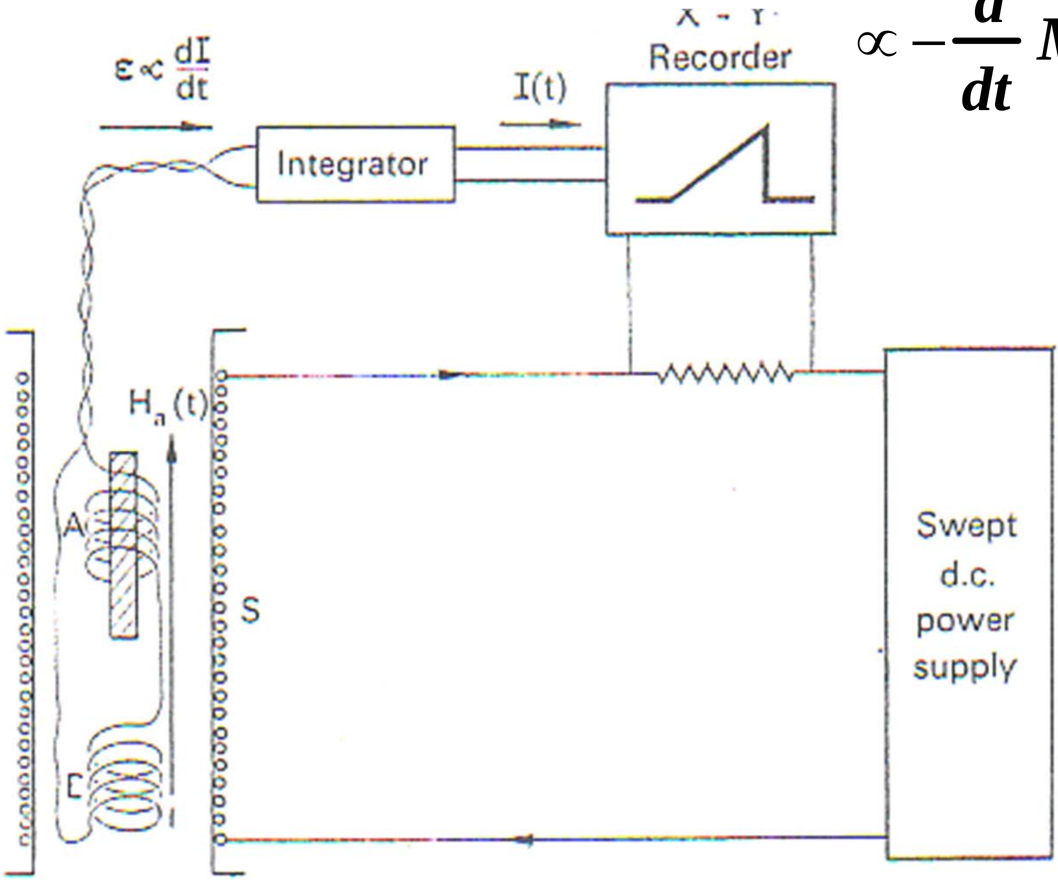

$$V_{out} \propto \int_0^t \frac{d}{dt} M dt = M$$

Hc measurement

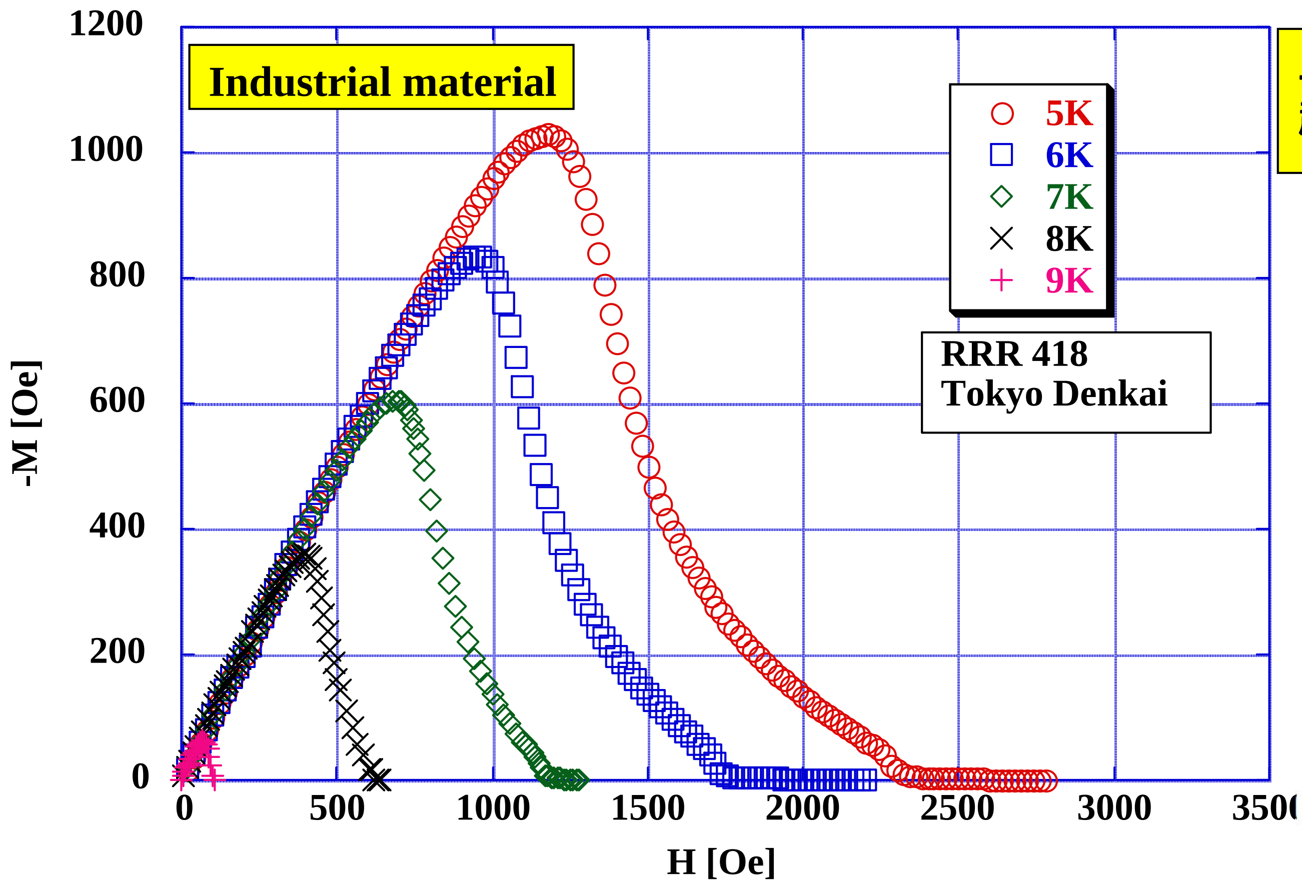

工業製産材の特性は、ラボの
超高純度の物とどう異なるか？

Lab material RRR~2000

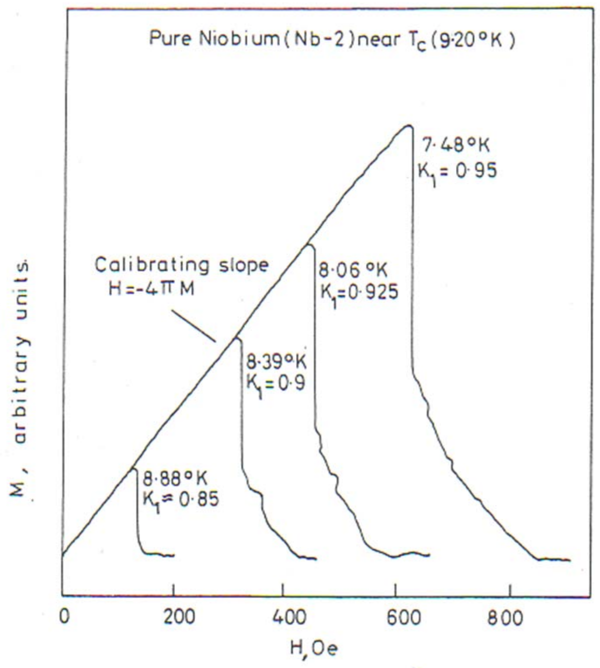

$$F_n - F_s = -\int_0^{Hc2} MdH = \frac{1}{2}\mu H_c^2$$

Example of demagnetization curve on Niobium
(NingXia, Large Grain RRR=340)

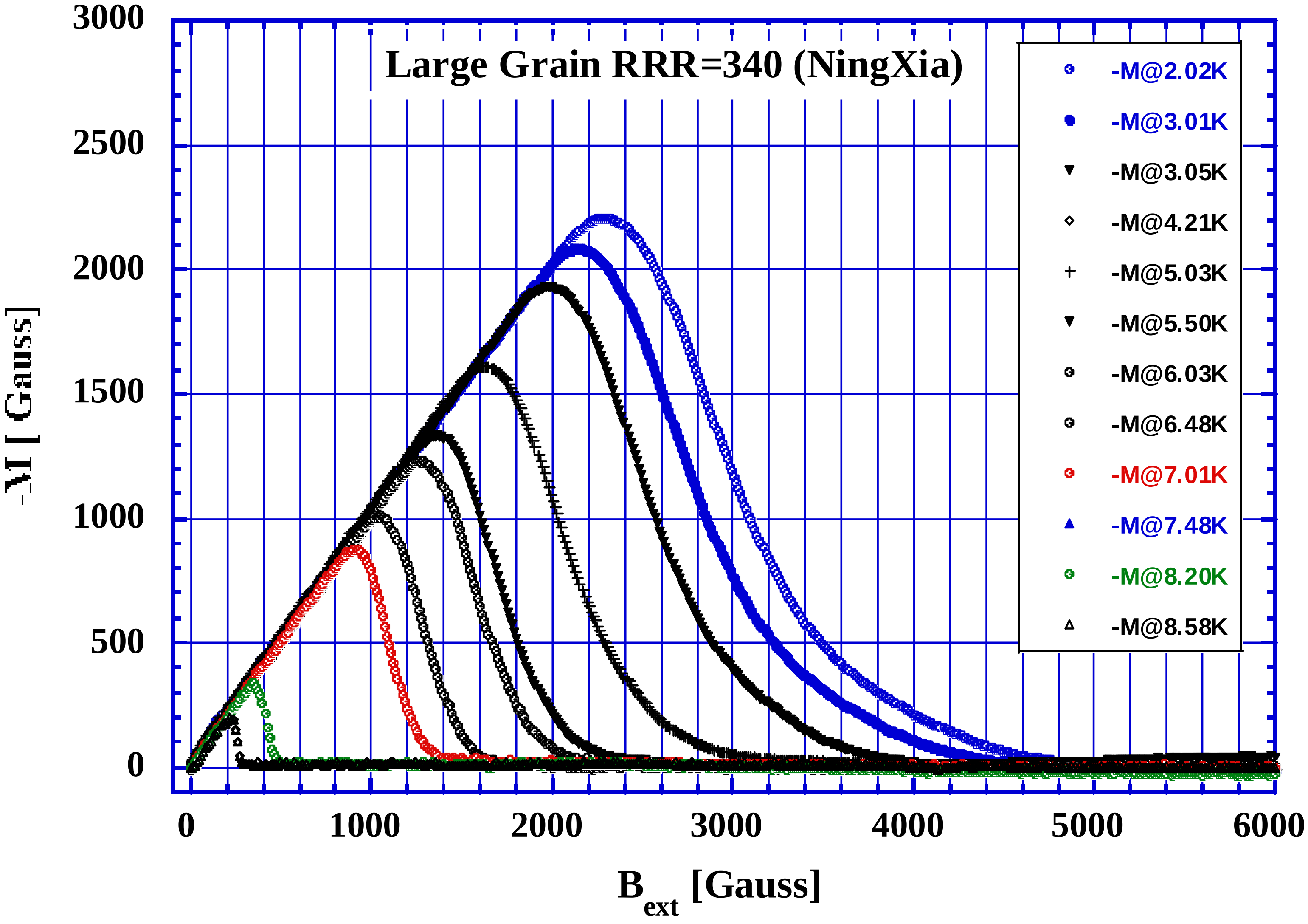

Measurement results with H_{C1}, H_C, H_{C2}

Lab Nb material

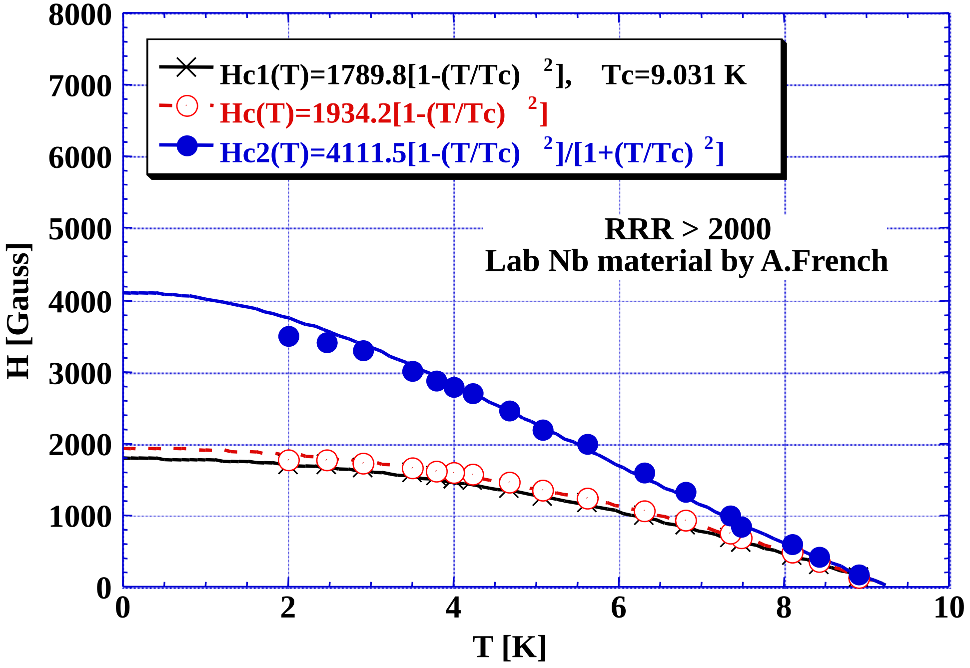

Industrial produced Nb material

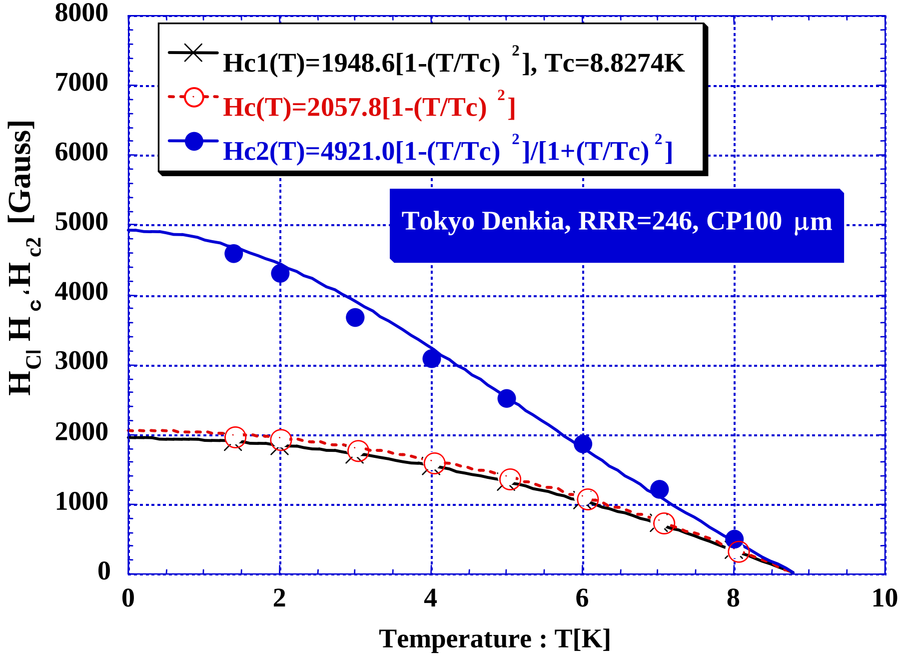

$$\mathbf{H_c(T)} = \mathbf{H_c}(0)\cdot\left[1-\left(\frac{\mathbf{T}}{\mathbf{T_c}}\right)^2\right],\quad \mathbf{F_n}-\mathbf{F_s} = -\int_0^{Hc2} MdH = \frac{1}{2}\mu \mathbf{H}_c^2$$

Abrikosov Theory: Type-II SCの理論

$$H_c = \frac{\kappa}{\lambda^2}\frac{\hbar c}{\sqrt{2}e^*} = \frac{\kappa}{\lambda^2}\frac{(hc/2e)}{2\pi\sqrt{2}} = \frac{\phi_0}{2\pi\sqrt{2}\lambda\xi}$$

$$H_{c2} = \sqrt{2}\frac{\lambda}{\xi}\frac{\phi_0}{2\pi\sqrt{2}\lambda\xi} = \frac{\phi_0}{2\pi\xi^2}$$

$$H_{c1} = \frac{\phi_o}{4\pi\lambda^2}\ln(\frac{\lambda}{\xi} + 0.08)$$

$$\phi_0 = hc/2e = 2.0678 \times 10^{-7} Gauss \cdot cm^2$$

$$= 2.0678 \times 10^{-15}\ T \cdot m^2$$

T-dependence of λ, ξ, κ

Abrikosov theory

$$\xi = \sqrt{\frac{\phi_o}{2\pi \cdot H_{c2}}}\ ,\quad \lambda = \sqrt{\frac{\phi_o \cdot H_{c2}}{4\pi \cdot H_c^{\,2}}}$$

一方、理論/実験の両面からλ(T)、Hc(T)は、$\lambda(T) = \dfrac{\lambda(0)}{\sqrt{1 - \left(\dfrac{T}{T_c}\right)^4}}$, $H_c(T) = H_c(0) \cdot \left[1 - \left(\dfrac{T}{T_c}\right)^2\right]$

$$\left\{\begin{aligned}
H_{c2}(T) &= \frac{4\pi\lambda(T)^2}{\phi_o} \cdot H_c(T)^2 = \frac{4\pi\lambda(0)^2 \cdot H_c(0)^2}{\phi_o} \cdot \frac{\left[1-(T/T_c)^2\right]^2}{1-(T/T_c)^4} \\
&= H_{c2}(0) \cdot \frac{1-(T/T_c)^2}{1+(T/T_c)^2} \\
\xi(T) &= \sqrt{\frac{\phi_o}{2\pi \cdot H_{c2}(0)}} \cdot \sqrt{\frac{1+(T/T_c)^2}{1-(T/T_c)^2}} = \xi(0) \cdot \sqrt{\frac{1+(T/T_c)^2}{1-(T/T_c)^2}} \\
\frac{\lambda(T)}{\xi(T)} &\equiv \kappa(T) = \frac{1}{\sqrt{2}} \cdot \frac{H_{c2}(T)}{H_c(T)} = \frac{H_{c2}(0)}{\sqrt{2} \cdot H_c(0)} \cdot \frac{1}{1+(T/T_c)^2} = \frac{\kappa(0)}{1+(T/T_c)^2}
\end{aligned}\right.$$

λ(T) fitting

Lab material, RRR>2000

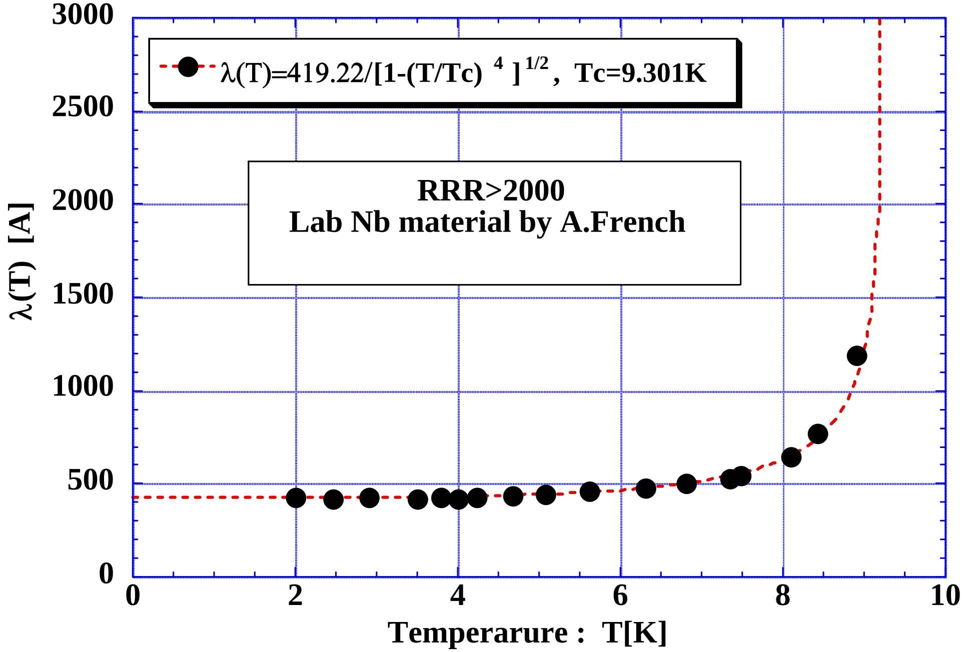

Industrial produced material

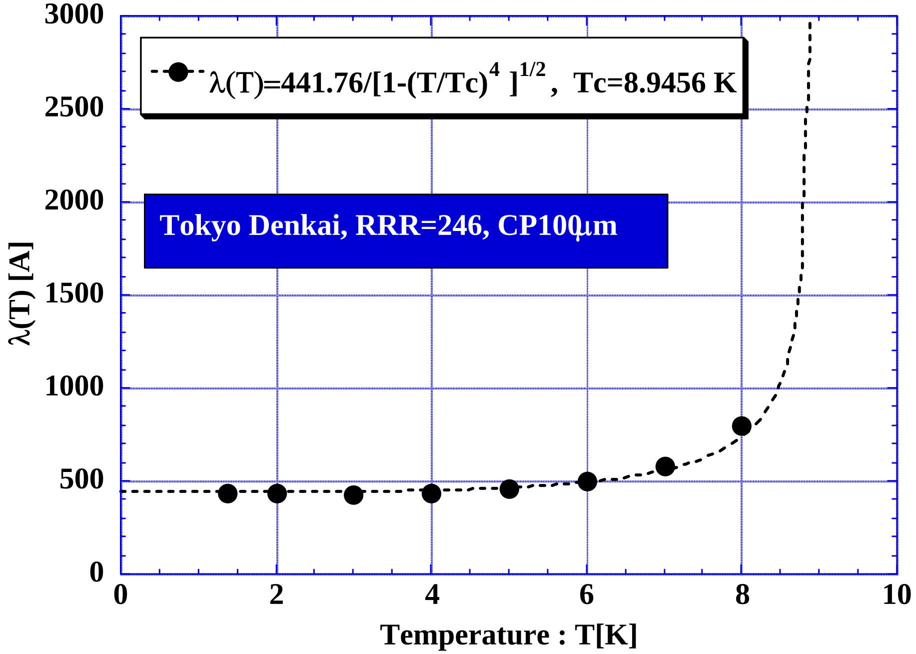

工業製産されたNb材でも理論通り

Hc Fitting

Lab material, RRR>2000

Industrial produced materail

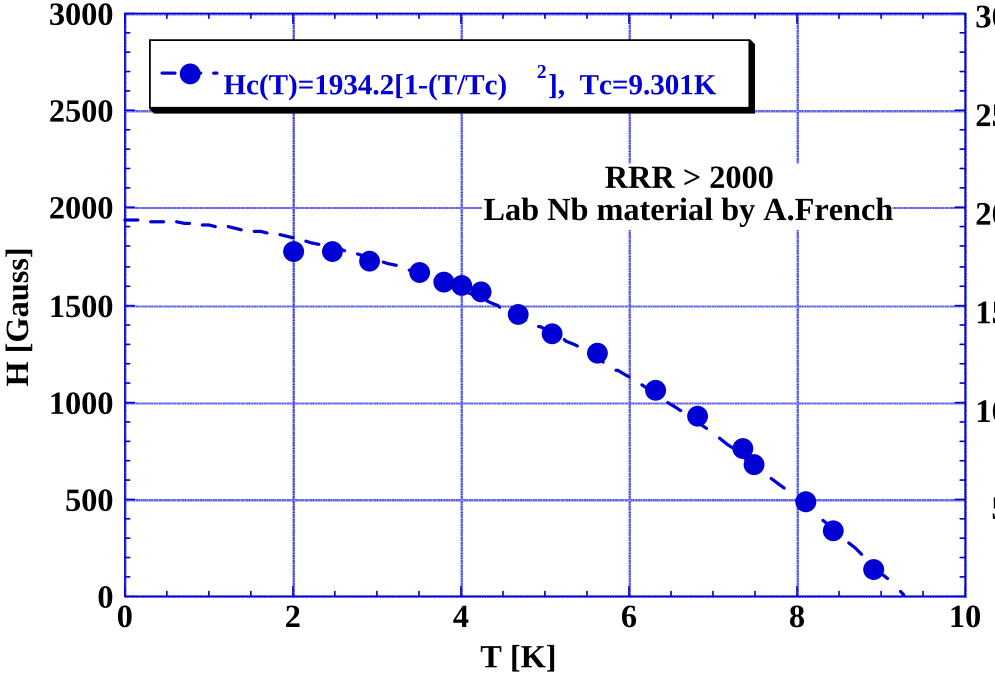

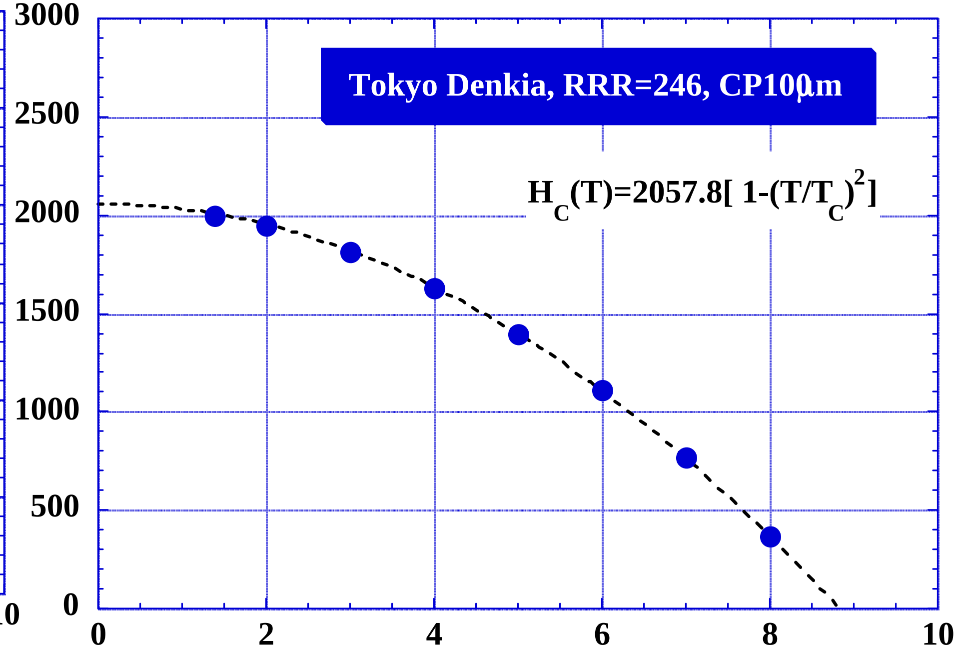

工業製産されたNb材でも理論通り

H_{C2}(T), ξ(T) fitting for Lab material, RRR>2000

$$H_{c2} \propto (1 - T/T_c) \quad \longleftarrow \quad \xi(T) \propto \frac{1}{\sqrt{1 - T/T_c}} \quad @\ \mathrm{T} \cong \mathrm{T_c}$$

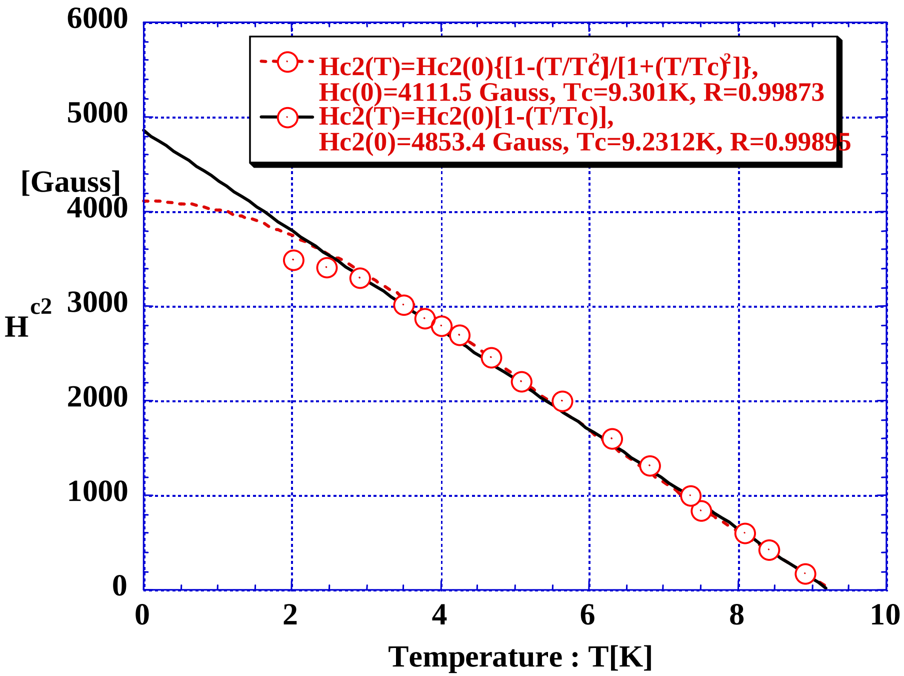

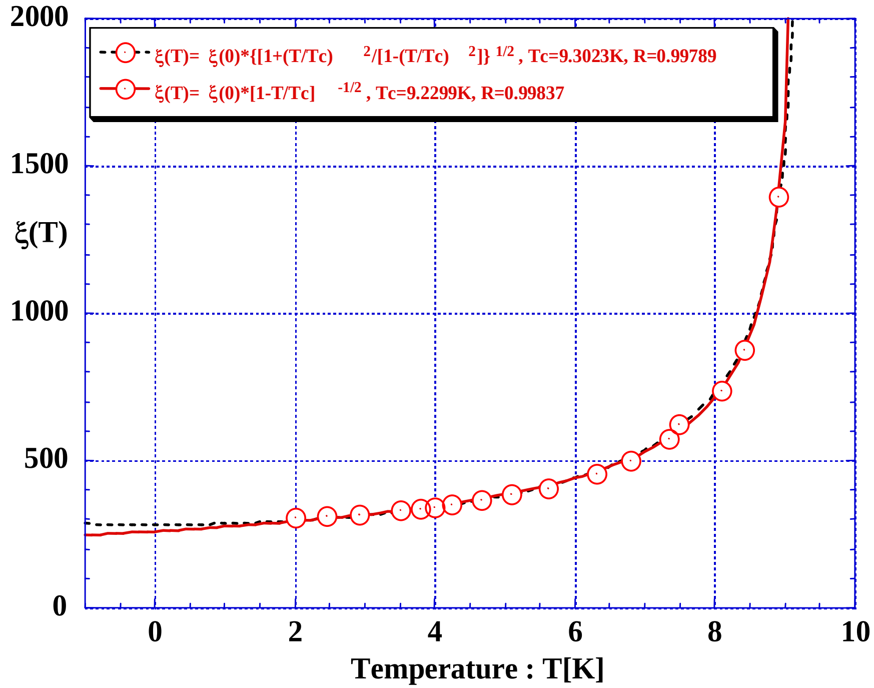

$$\xi(0) \cdot \sqrt{\frac{1 + (\mathrm{T}/\mathrm{T_c})^2}{1 - (\mathrm{T}/\mathrm{T_c})^2}}$$

この式の方がconsistent。

H_{C2} and ξ fitting for industrial material

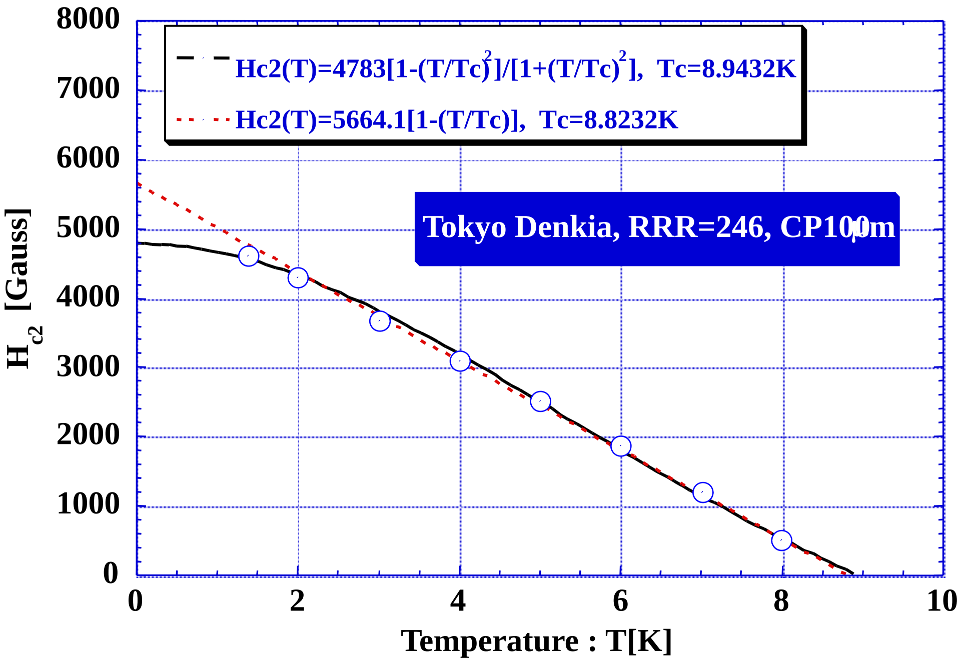

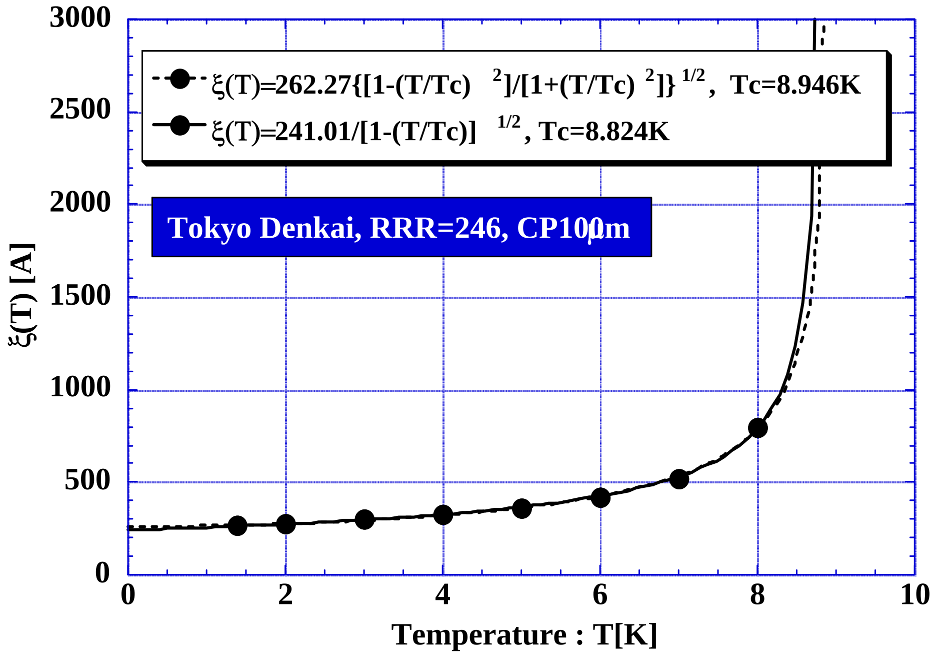

$$\xi(T) = \xi(0)\cdot\sqrt{\frac{1+(T/T_c)^2}{1-(T/T_c)^2}}$$ 、 $$\xi(T) = \frac{\xi(0)}{\sqrt{1-T/T_c}}$$ 共に実験結果をfitする。

しかし、後者はTcが小さいのでここでは、前者を使う。

T-dependence of κ with Lab material

Nb
Lab material
RRR>2000

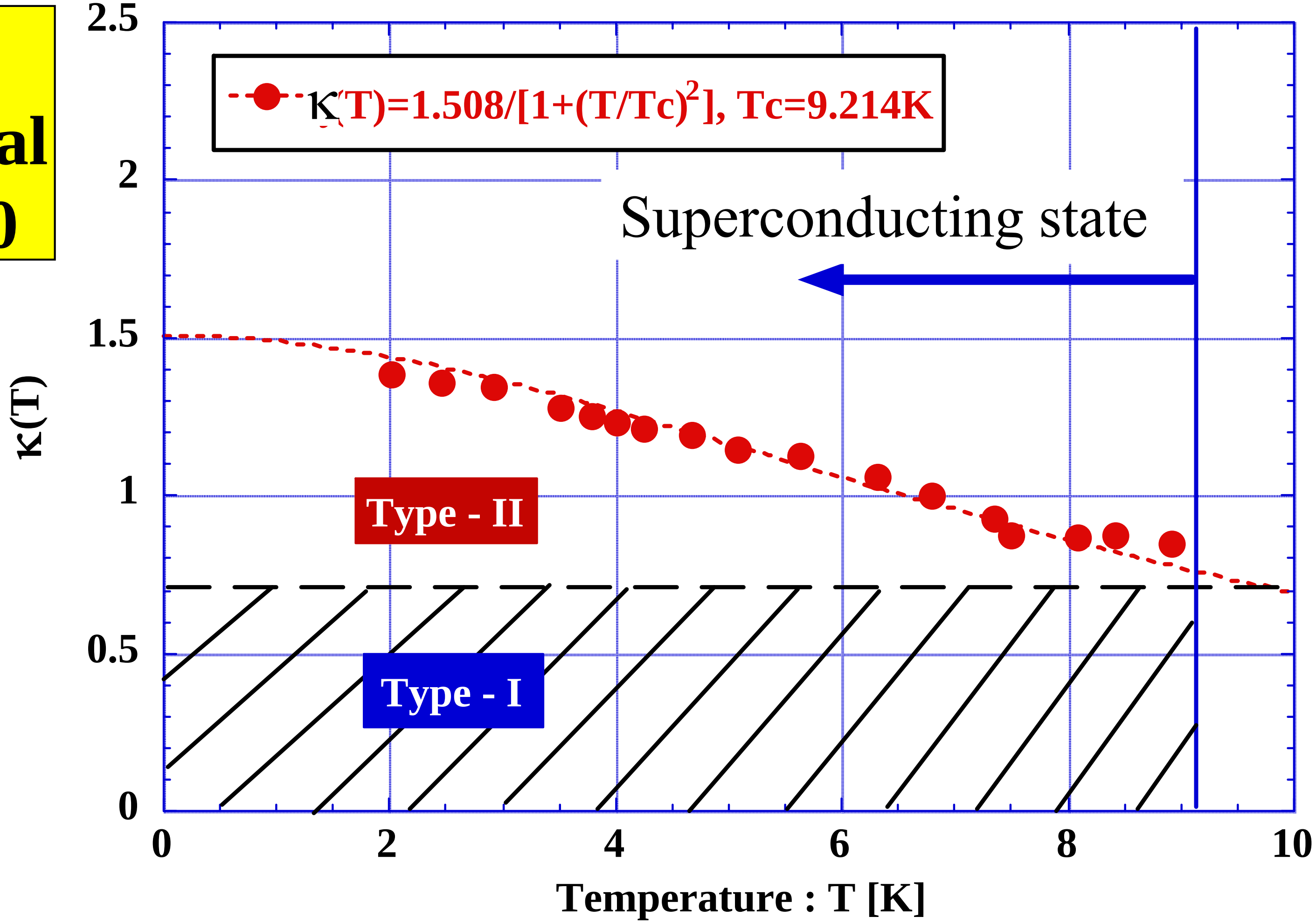

T dependence of κ with industrial material

RRR=246

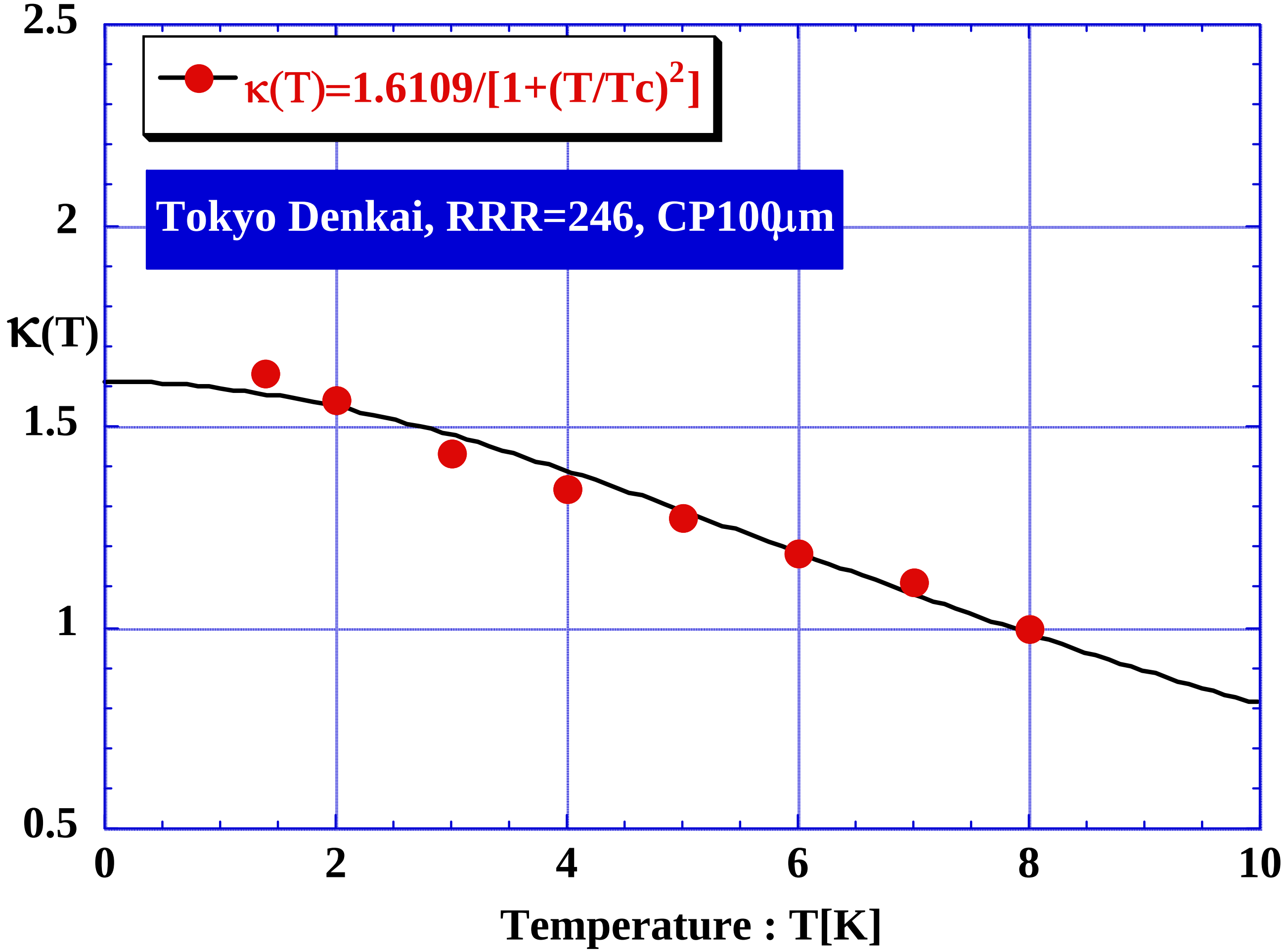

Thermal conductivity measurement

Normal conductor : $\kappa_{en} = \dfrac{1}{W_{en}} = \left[\dfrac{\rho}{L_O T} + aT^2 \right]^{-1}$

$\rho = \dfrac{\rho_{300K}}{RRR}$ e-impurities scatt.

e-lattices scatt.

Wiedemann-Franz low:

$\kappa_e = \dfrac{\pi^2 n k_B^2 \tau}{3m} \cdot T, \quad \dfrac{\kappa_e}{\sigma} = \dfrac{\pi^2}{3}\left(\dfrac{k_B}{e}\right)^2 \cdot T = L_O T$

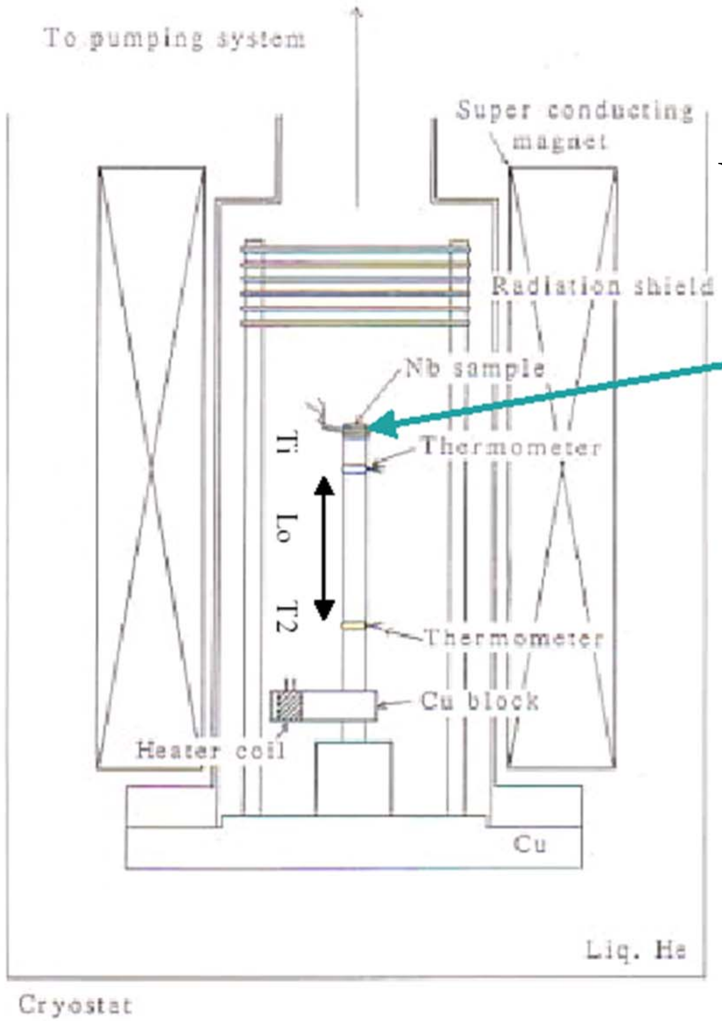

$$P[w] = S(m^2) \cdot \kappa(T) \cdot \frac{T_1(K) - T_2(K)}{L_O(m)}$$

$$T \equiv \frac{T_1 + T_2}{2}, \ S\text{: area of cross-section}$$

$$\kappa(T) = \frac{P}{S} \cdot \frac{L_O}{T_1 - T_2} \qquad \left[\frac{w}{m \cdot K}\right]$$

Thermal conductivity of Nb material at low temperature

Boltzmann 統計：energy Δ, Temp. T での存在確率

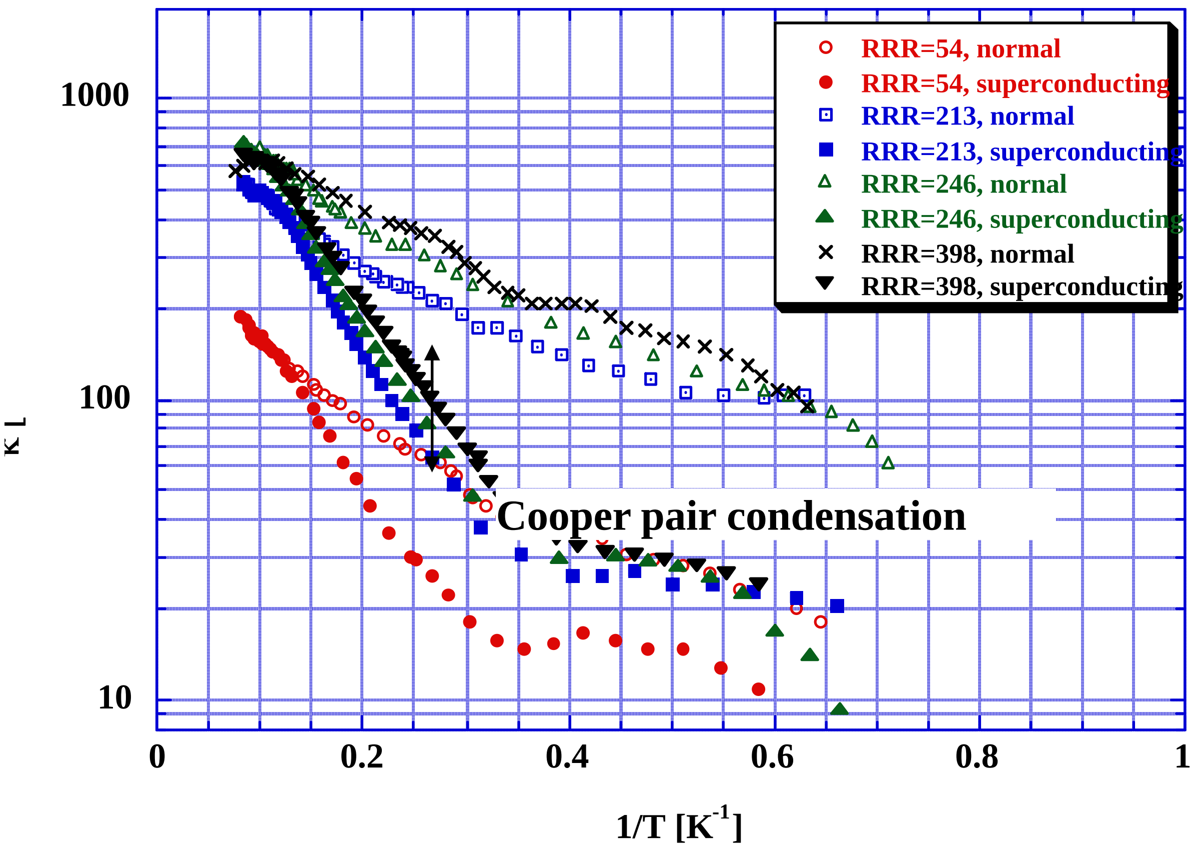

$$\exp(-\frac{\Delta}{k_B \cdot T})$$

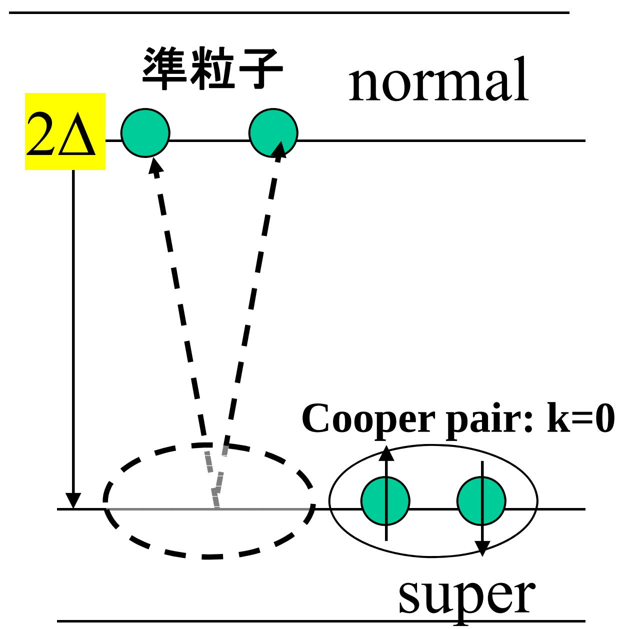

Thermal conductivity comparison with NC and SC

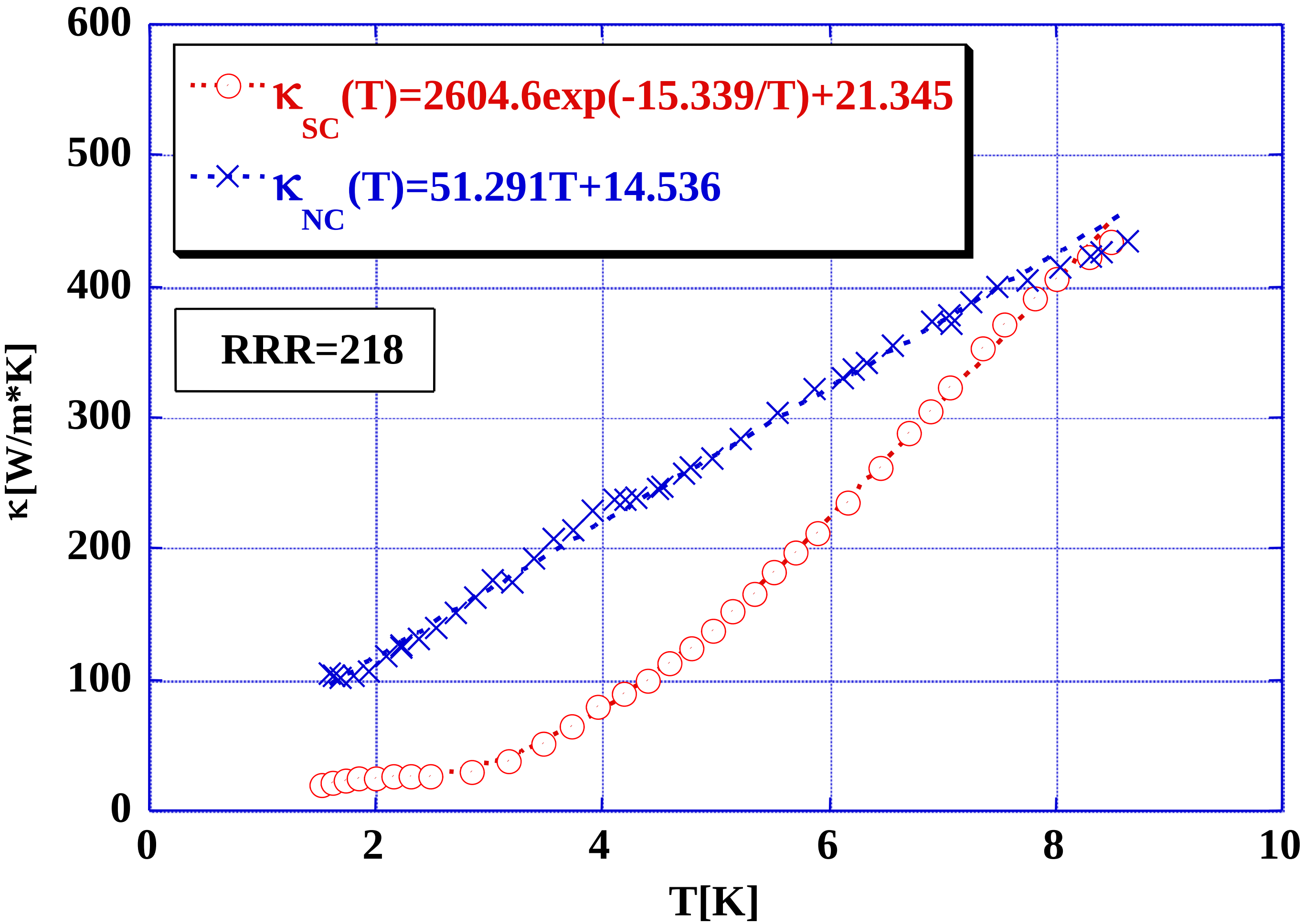

$$\frac{\Delta}{k_B} = 15.339$$

$$\Downarrow$$

$$\frac{2\Delta}{k_B T_c} = \frac{2 \times 15.339}{k_B\, 9.25}$$

$$2\Delta = 3.317 k_B T_c$$

BCS theory

$$2\Delta = 3.52 k_B T_c$$

Calculation of thermal conductivity based on Quantum mechanics

$$\kappa_s(T) = R(y)\cdot\left[\frac{\rho_{295K}}{L\cdot RRR\cdot T} + a\cdot T^2\right]^{-1} + \left[\frac{1}{D\cdot \exp(y)\cdot T^2} + \frac{1}{BlT^3}\right]^{-1}$$

e - impurities scatt.   e - phonons scatt.   lattice - phonnons scatt.   lattice - grain boundaries scatt.

$L = 2.05E-8,\ RRR = 200,\ \rho_{295K} = 14.5E-8\ \Omega m,\ a = 7.52E-7$

$-y = \alpha\cdot\frac{T_c}{T},\ \alpha = 1.53,\ T_c = 9.25K,\ T \le 0.6\cdot T_c$

$D = 4.27E-3,\ B = 4.34E3,\ l = 50\mu m$

$$R(y) = \frac{\kappa_{es}}{\kappa_{en}} = \frac{2F_1(-y) + 2y\ln(1+e^{-y}) + \dfrac{y^2}{(1+e^{y})}}{2F_1(0)},$$

$$F_n(-y) = \int_0^\infty \frac{z^n}{1+e^{z+y}}dz$$

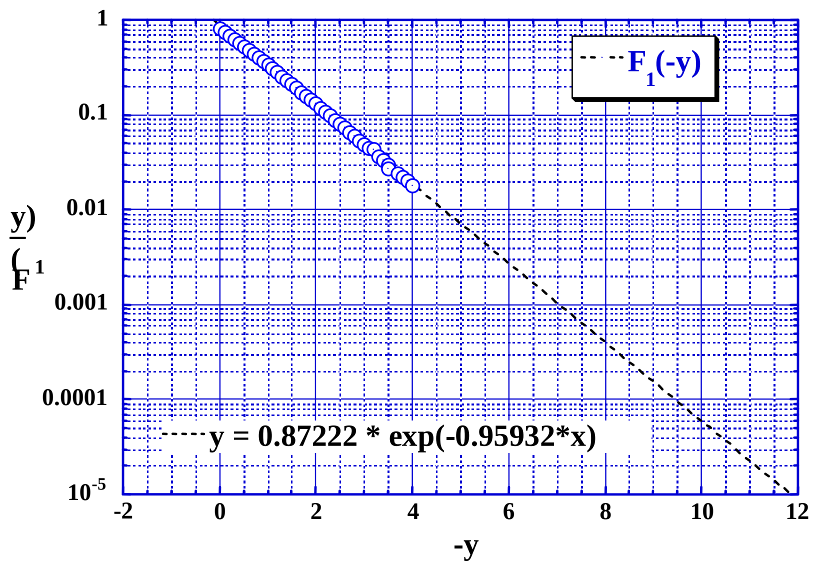

Calculated κ_{sc}(T)

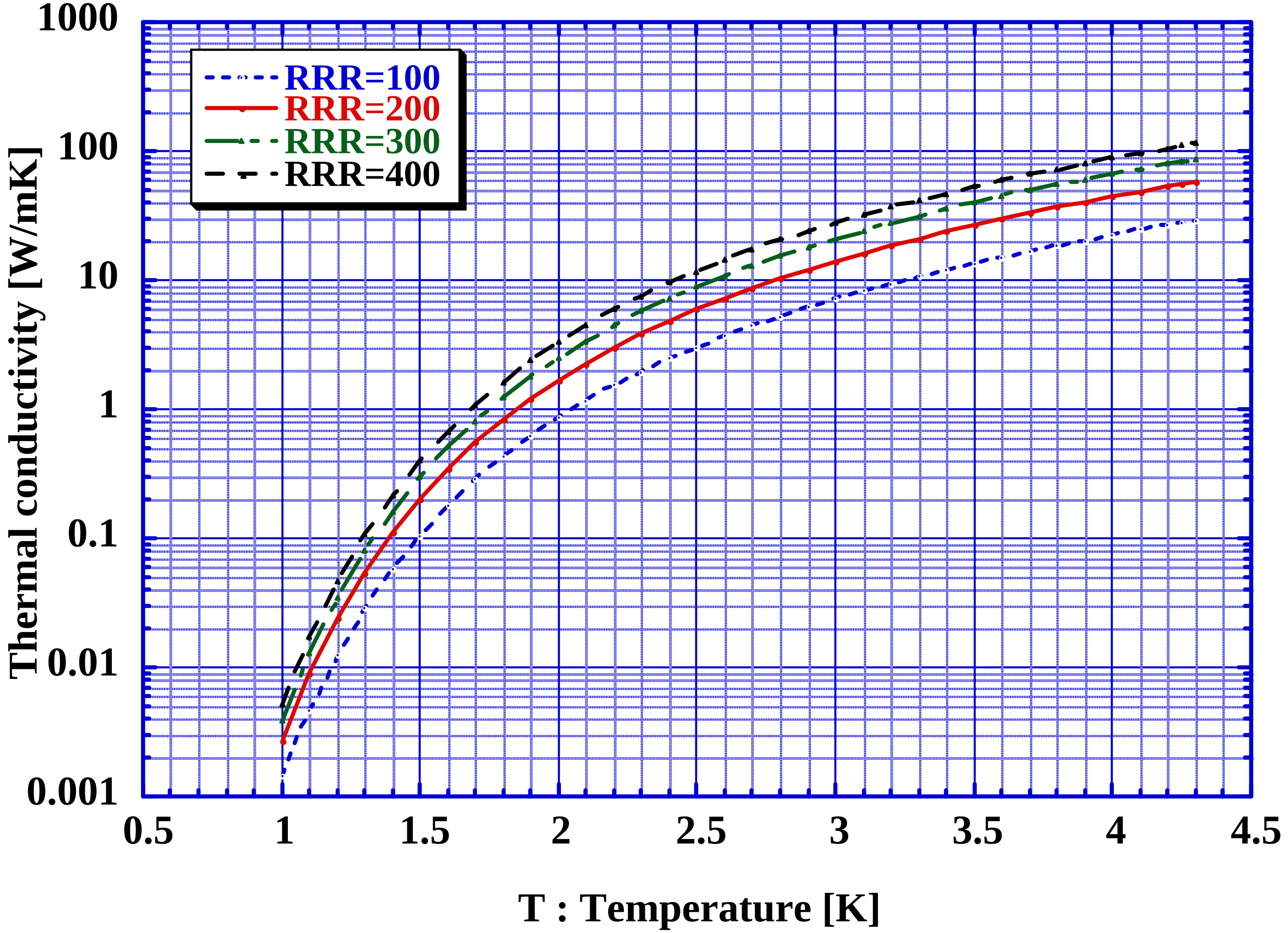

Nbの2Kでの熱伝導率はSUS304(常温, 15W/m*K)）の～1/15、純銅（4.2K, 6800W/m*K)の1/6800。

Kapitza Resistance

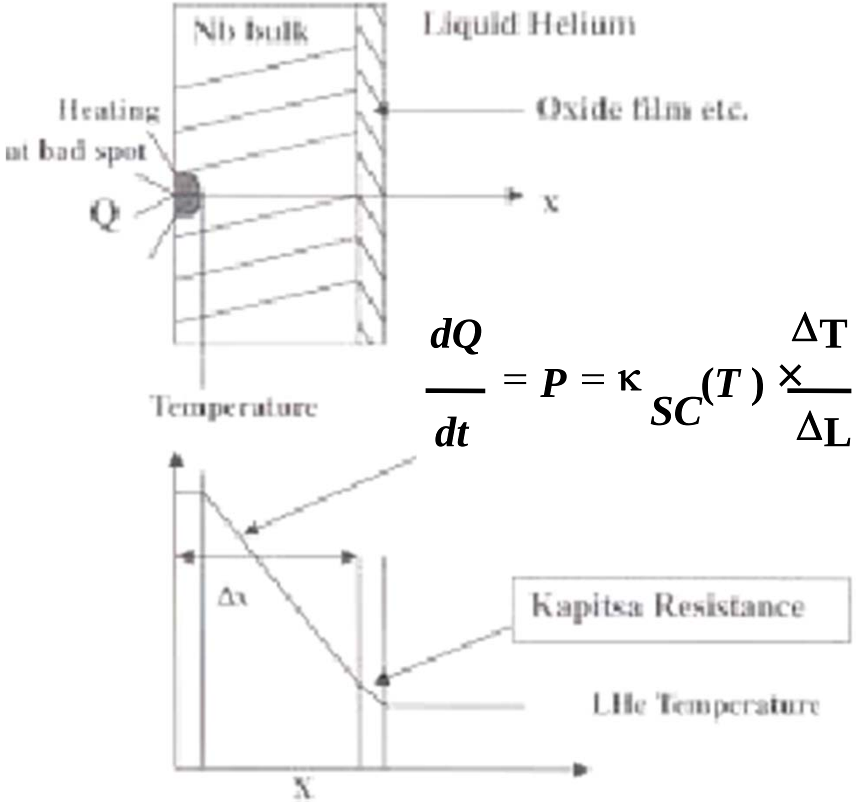

$$\frac{dQ}{dt} = P = \kappa_{SC}(T) \times \frac{\Delta T}{\Delta L}$$

$$h_k(T) = 705.51 \cdot T^{3.7113}$$

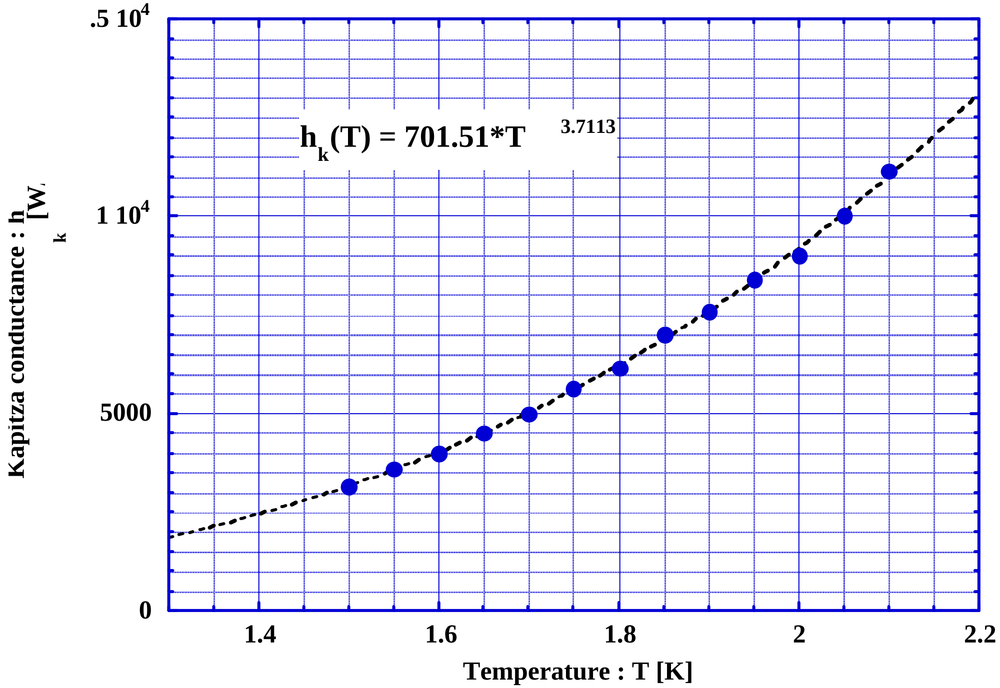

$$\Delta T = P \cdot \left\{ \frac{d}{\kappa_{SC}(\tilde{T})} + \frac{1}{h_k(\tilde{T})} \right\}$$

Kapitza resistanceの影響は小さい。

RRR measurement

非常に簡単な測定!! 熱伝導率に比例する。

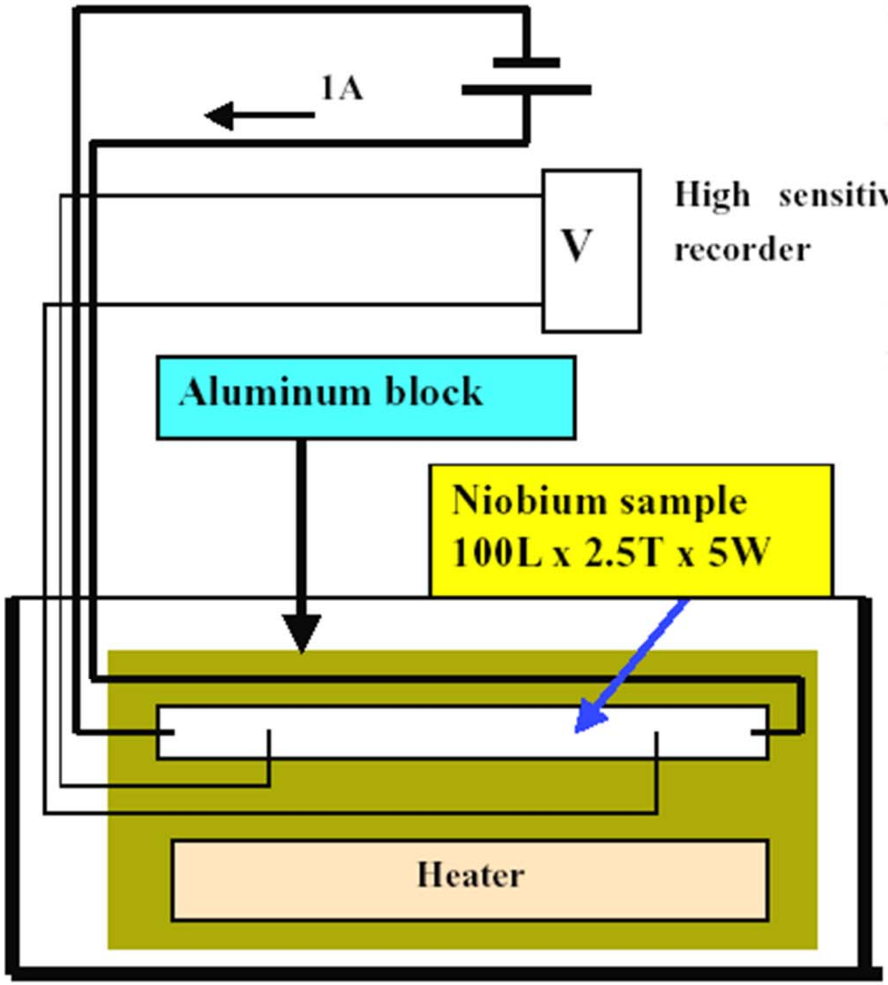

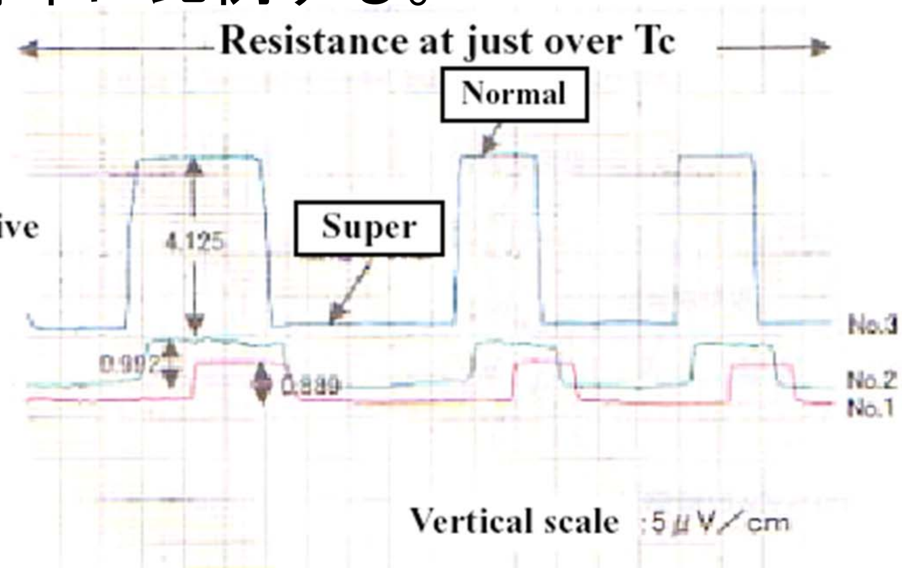

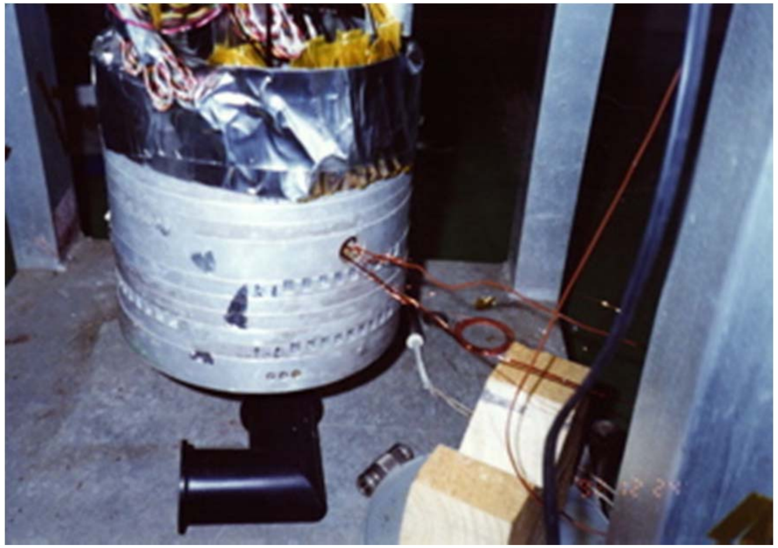

$$RRR \equiv \frac{R_{300K}}{R_{9.5K}}$$

Linear relationship between κ_{sc} (2K, 4.25K) and RRR

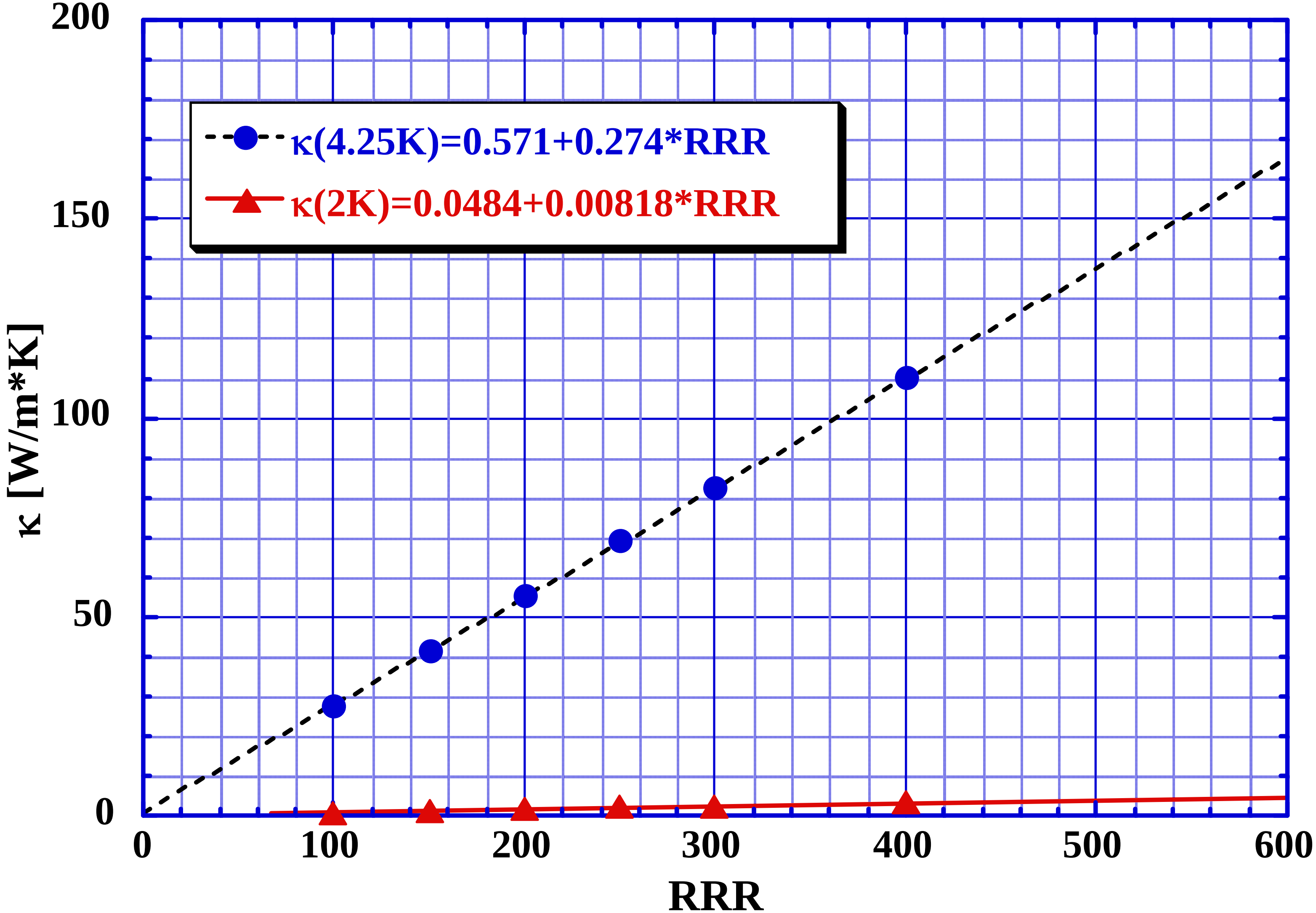

Surface resistance of metal in RF application

導体内(ε、μ、ρ＝0)の電磁波

Maxwell Eqs.

$$\nabla\cdot\vec{\mathbf{B}}=0\,,\ \nabla\times\vec{\mathbf{E}}+\mu\frac{\partial\vec{\mathbf{H}}}{\partial\mathbf{t}}=0$$

$$\nabla\cdot\vec{\mathbf{D}}=0\,,\ \nabla\times\vec{\mathbf{H}}-\varepsilon\frac{\partial\mathbf{E}}{\partial\,\mathbf{t}}-\sigma\vec{\mathbf{E}}=\mathbf{0}$$

$$\vec{\mathbf{J}}=\sigma\vec{\mathbf{E}}\ \textbf{(Ohm's law)}$$

E, Hがzと時間のみ関数。縦（longitudinal)、横(transverse)に分けて

$$\vec{\mathbf{E}}=\vec{\mathbf{E}}_{\ell}(\mathbf{z,t})+\vec{\mathbf{E}}_{\mathbf{t}}(\mathbf{z,t}),\ \vec{\mathbf{H}}=\vec{\mathbf{H}}_{\ell}(\mathbf{z,t})+\vec{\mathbf{H}}_{\mathbf{t}}(\mathbf{z,t})$$

Maxwell Eqs.　div. から

$$\frac{\partial\mathbf{H}_{\ell}}{\partial\mathbf{Z}}=0\ (\because\nabla\ \vec{\mathbf{B}}=\mathbf{0})\rightarrow\frac{\partial\mathbf{H}_{\ell}}{\partial\ \mathbf{t}}=0$$

⇒ $\vec{\mathbf{H}}$の縦成分(z成分)は、静磁場の場合のみ$\neq 0$

$$\frac{\partial\mathbf{H}_{\ell}}{\partial\mathbf{Z}}=0\,,\ \left(\frac{\partial}{\partial\,\mathbf{t}}+\frac{\boldsymbol{\sigma}}{\boldsymbol{\varepsilon}}\right)\mathbf{E}_{\ell}=0$$

⇒ $\mathrm{E}_{\ell}(x,t)=\mathrm{E}_{o}e^{-\sigma\cdot t/\varepsilon}$　すぐ減衰する

横成分

$\vec{\mathbf{E}}_t = \vec{\mathbf{E}}_o \exp(i\vec{\mathbf{k}}\cdot\vec{\mathbf{x}} - i\omega t)$ ：平面波を仮定

Maxwell eqs.の第一回転の式から $\vec{\mathbf{H}}_t = \dfrac{1}{\mu\omega}\left(\vec{\mathbf{k}}\times\vec{\mathbf{E}}_t\right)$

第二回転の式から $i\left(\vec{\mathbf{k}}\times\vec{\mathbf{H}}_t\right) + i\varepsilon\omega\vec{\mathbf{E}}_t - \sigma\vec{\mathbf{E}}_t = 0$

$\mathbf{E}_t$または$\mathbf{H}_t$を消去して

$$\left[\mathbf{k}^2 - \left(\mu\varepsilon\omega^2 + i\mu\omega\sigma\right)\right]\begin{Bmatrix}\vec{\mathbf{E}}_t \\ \vec{\mathbf{H}}_t\end{Bmatrix} = 0$$

$$\mathbf{k}^2 = \mu\varepsilon\omega^2\left(1 + i\frac{\sigma}{\omega\varepsilon}\right)$$

$$k = \alpha + i\beta$$

$$\begin{Bmatrix}\alpha \\ \beta\end{Bmatrix} = \sqrt{\mu\varepsilon}\,\omega\left[\frac{\sqrt{1+\left(\dfrac{\sigma}{\omega\varepsilon}\right)^2} \pm 1}{2}\right]^{1/2}$$

$$\frac{\sigma}{\omega\varepsilon} >> 1$$:良導体の場合

$$k \approx (1+i)\sqrt{\frac{\mu\sigma\omega}{2}}$$

Skin depth : $\delta = \dfrac{1}{\beta} = \sqrt{\dfrac{2}{\mu\sigma\omega}}$

Surface Impedance

$$\vec{\mathbf{H}}_{\mathbf{t}} = \frac{1}{\mu\omega}\vec{\mathbf{k}}\times\vec{\mathbf{E}}_{\mathbf{t}}$$

kと$\mathbf{E}_t$は直行している。

Surface impedance : $Z \equiv R_s + iX_s \equiv \dfrac{E_t}{H_t} = \dfrac{\mu\omega}{k}$

良導体の場合 $k = (1+i)\sqrt{\dfrac{\mu\sigma\omega}{2}}$

$$Z = \mu\omega\sqrt{\frac{2}{\mu\sigma\omega}}\cdot\frac{1}{1+i} = \mu\omega\sqrt{\frac{2}{\mu\sigma\omega}}\cdot\frac{1-i}{2} = (1-i)\sqrt{\frac{\mu\omega}{2\sigma}}$$

$$\boxed{\mathbf{R_s} = \sqrt{\frac{\mu\omega}{2\sigma}} = \frac{1}{\sigma}\sqrt{\frac{\mu\sigma\omega}{2}} = \frac{1}{\sigma\delta}}$$

Frequency dependence of δ and Rs with copper cavity

Frequency	δ[μm]	Rs [mΩ]	Comment
508MHz	2.90	5.78	トリスタン
1300MHz	1.81	9.24	TESLA
2856MHz	1.22	13.70	Conventional LINAC
11.4GHz	0.61	27.36	GLC

周波数が高くなるほど、skin depthが浅くなり、

空洞性能が表面状態に敏感になる。

AC surface resistance in superconductor-Two Fluid model

General equation: $m\frac{\partial \vec{v}}{\partial t} = q(\vec{E} + \vec{v} \times \vec{B}) - m\vec{v}\nu$

Two -fluid model

$\vec{J} = \vec{J}_s + \vec{J}_n\ ,\ \vec{J}_s = n_s q_s \vec{v}_s\ ,\ \vec{J}_n = n_n q_n \vec{v}_n$

Maxwell equation: niglecting the Lorentz term, $\vec{v} \times \vec{B} << 1$

$$m_s \frac{\partial \vec{v}_s}{\partial t} = q_s \vec{E},\ m_s = 2m_e,\ q_s = 2 \cdot (-e)$$

$$m_e \frac{\partial \vec{v}_n}{\partial t} = q_n \vec{E} - m_e \nu \vec{v}_n\ ,\ q_n = -e$$

$$\vec{E} = \vec{E}_o e^{i\omega t} \Rightarrow \vec{J}_s = \frac{n_s q_s^2}{i\omega m_s}\vec{E}\ ,\quad \vec{J}_n = \frac{n_n e^2}{i(\omega - i\nu)}\vec{E}$$

$$\vec{J} = \left(\frac{n_s q_s^2}{i\omega m_s} + \frac{n_n e^2}{i(\omega - i\nu)m_e}\right)\vec{E}$$

$$\nu > \omega \Rightarrow \vec{J} = \left(\frac{n_n e^2}{\nu m_e} - i\frac{n_s q_s^2}{\omega m_s}\right)\vec{E} = (\sigma_n - i\sigma_s)\vec{E} = \sigma\vec{E}$$

$$\boxed{\sigma = \sigma_n - i\sigma_s}$$

$$Z = (1-i)\sqrt{\frac{\mu\omega}{2\sigma}} = (1-i)\sqrt{\frac{\mu\omega}{2(\sigma_n - i\sigma_s)}}$$

$$= (1-i)\sqrt{\frac{\mu\omega}{2}} \cdot \frac{1}{\sqrt{-i\sigma_s(1-\sigma_n / i\sigma_s)}}$$

$$\approx (1-i)\sqrt{\frac{\mu\omega}{2}} \cdot \frac{(1+\dfrac{\sigma_n}{i2\sigma_s})}{\sqrt{-i\sigma_s}}$$

$$= \sqrt{\mu\omega}\left(\frac{\sigma_n}{2\sigma_s^{3/2}} + i\frac{1}{\sigma_s^{1/2}}\right) \qquad \because \sqrt{-i} = \sqrt{e^{-\frac{\pi}{2}}} = \frac{(1-i)}{\sqrt{2}}$$

$$\boxed{Z = \frac{\mu\omega\lambda^3}{\delta^2} + i\mu\omega\lambda = \frac{\mu^2\omega^2\lambda^3\sigma_n}{2} + i\omega\mu\lambda}$$

ここで、 $\lambda = \sqrt{\dfrac{m_s}{n_s q_s^2 \mu}} = c\sqrt{\dfrac{2m}{4n_s\mu e^2}} = c\sqrt{\dfrac{m}{2n_s\mu e^2}}$

Surface resistance in superconductor

$$\sigma_n = \frac{n_n \cdot e^2 \cdot l}{m \cdot v_F} = \frac{e^2 \cdot l}{m \cdot v_F} \cdot n_s(T=0) \cdot e^{-\frac{\Delta}{k_B \cdot T}}$$

$$R_S = \frac{1}{2} \cdot (2\pi)^2 \cdot \mu^2 \cdot f^2 \cdot \lambda_L^3 \cdot l \cdot \frac{n_s(0)}{m v_F} \cdot e^{-\frac{\Delta}{k_B T}}$$

$$= A \cdot f^2 \cdot e^{-\frac{\Delta}{k_B T}}$$

BCS theory

$$R_{BCS}(T,\omega) = A(\lambda, \xi, \ell, Tc) \cdot \frac{f^2}{T} \cdot e^{-\frac{\Delta}{k_B T}}$$

At a finite temperature T

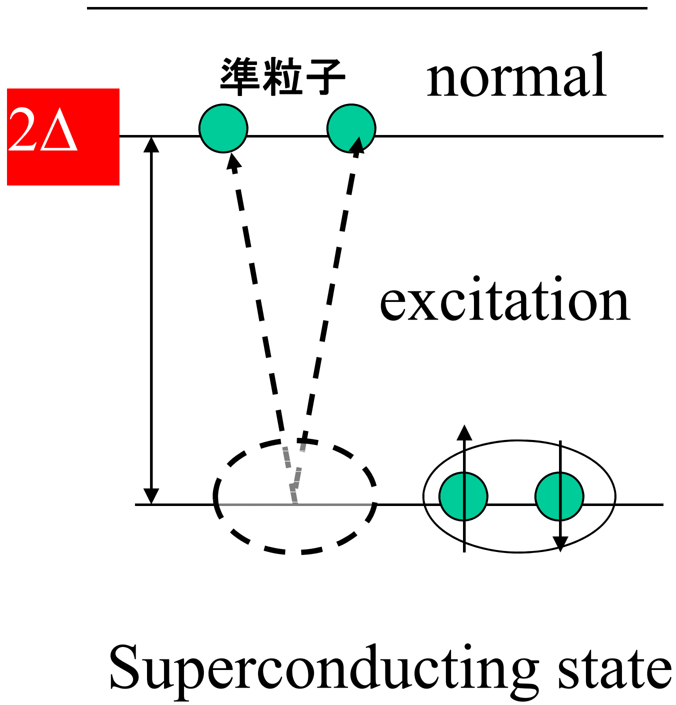

Calculation of R_{BCS}

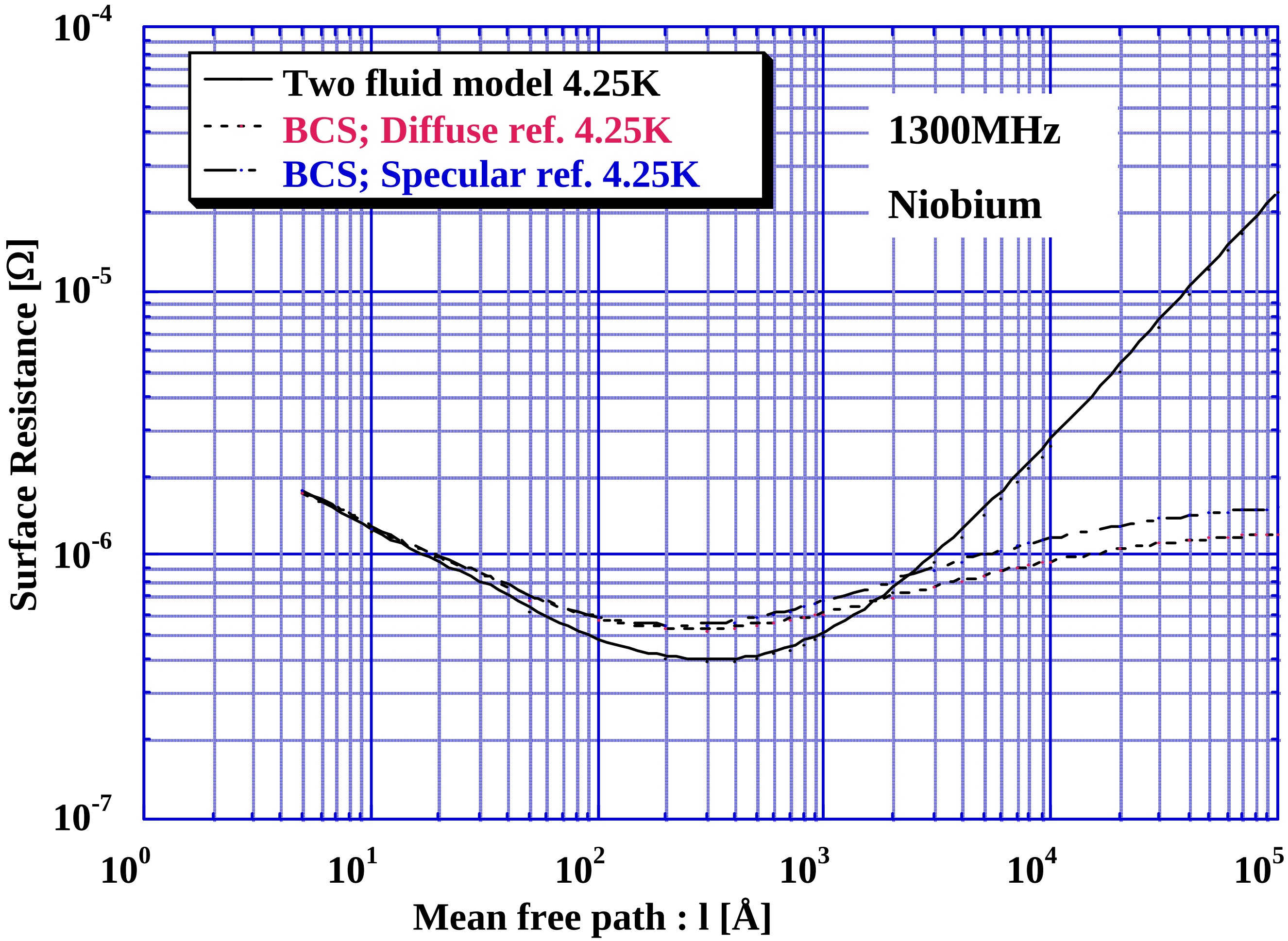

Mean free path(ℓ)に対するRsの一見不思議な振るまい

$\ell \approx$ **200 ~ 300** Å で最小値をとる。

$\ell[A] = 20 \cdot$ **RRR**

$$\lambda_L(l) = \lambda_L(l=\infty)\cdot\sqrt{1+\frac{\xi_o}{l}},\quad R_S(TF\ model) \propto \left(1+\frac{\xi_o}{l}\right)^{\frac{3}{2}}\cdot l,\quad l \ll 1, R_S \to \frac{\xi_o^{\frac{3}{2}}}{\sqrt{l}},\quad l \gg 1, R_s \to l$$

R_{BCS} at 2K

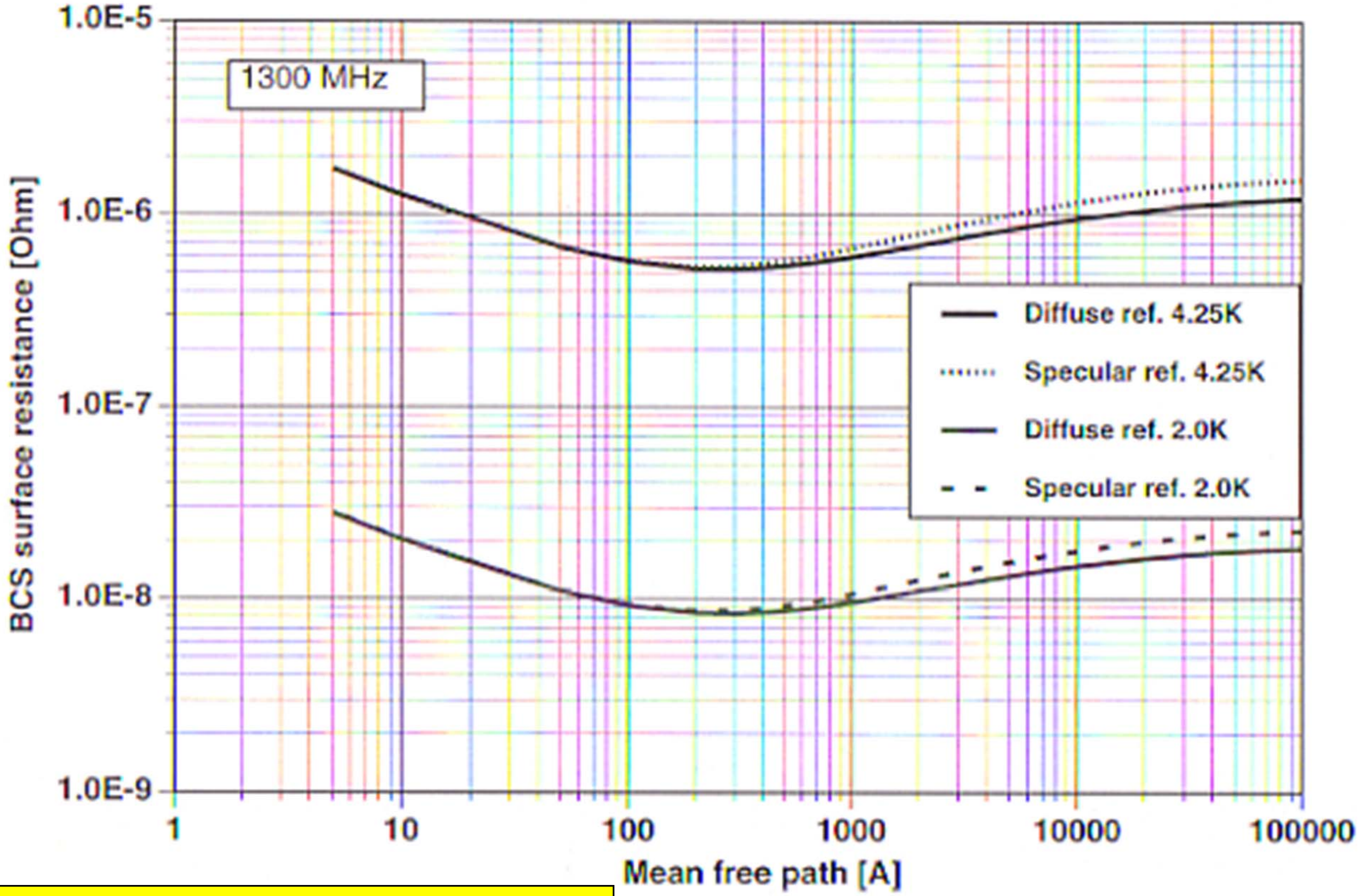

R_{BCS} ~ 8nΩ @ 2K, 1300MHz

Measurement of the Surface resistance

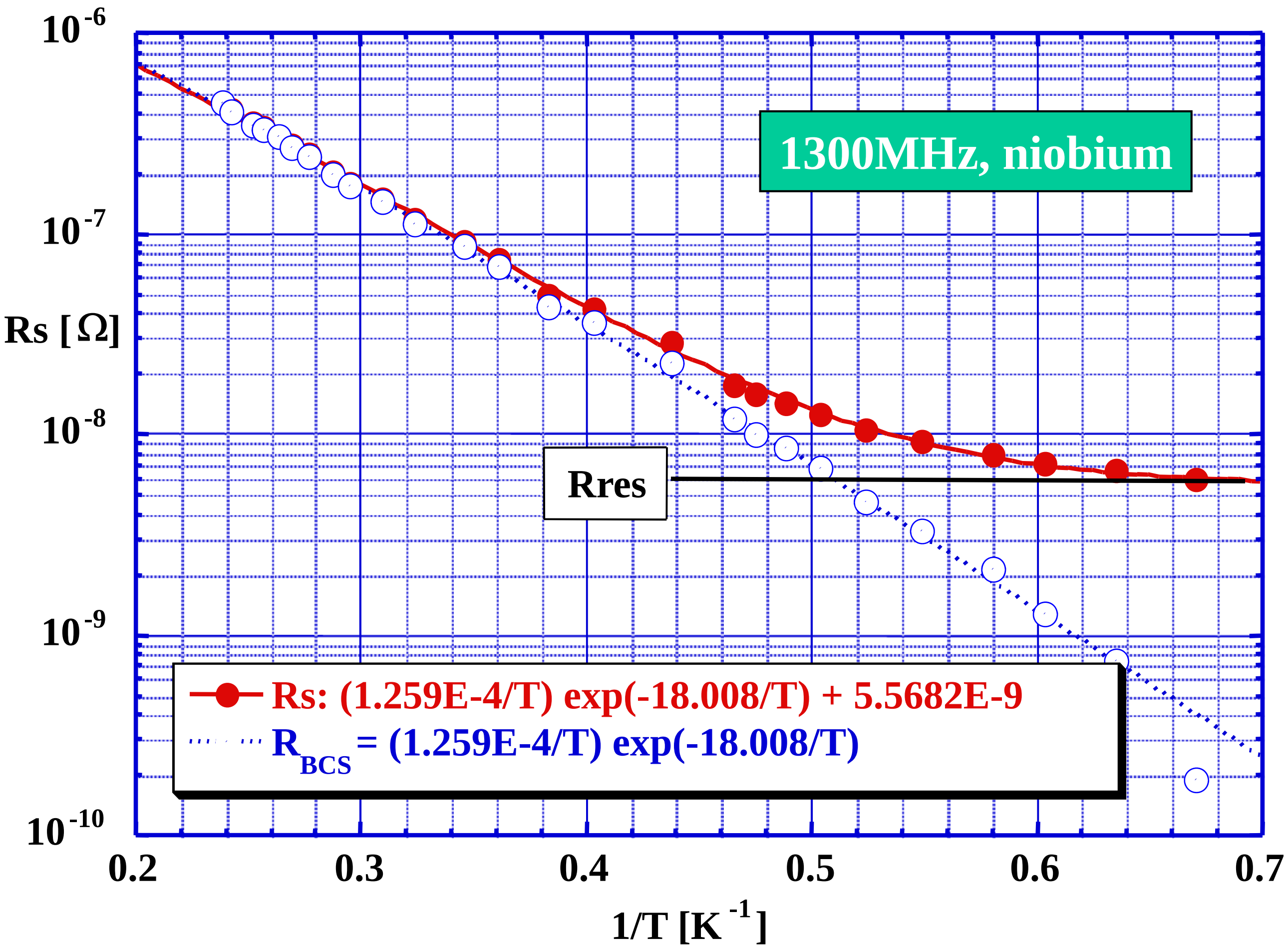

$$\frac{\Delta}{k_B} = 18.008 \Rightarrow \frac{2\Delta}{k_B T_c} = \frac{2 \cdot 18.008}{9.25} = 3.89$$

$$\frac{2\Delta}{k_B T_c} = 3.52 \text{ (BCS theory)}$$

表面状態、冷却中のcryostatの残留磁場等による。

$R_{BCS} \sim 8n\Omega$,
理論と良く合っている。

Real surface resistance : $R_S = R_{BCS}(T) + Rres$

Critical field limitation in SRF application

Vortex plane nucleation | **H:実効値** | **Vortex line nucleation**

Vortex plane nucleation

$$\frac{1}{2}\mu H^2 \cdot \lambda - \frac{1}{2}\mu H_c^2 \cdot \xi = 0$$

$$\boxed{H_c^{Plane} = \sqrt{\frac{\xi}{\lambda}} H_c = \frac{H_c}{\sqrt{\kappa}}}$$

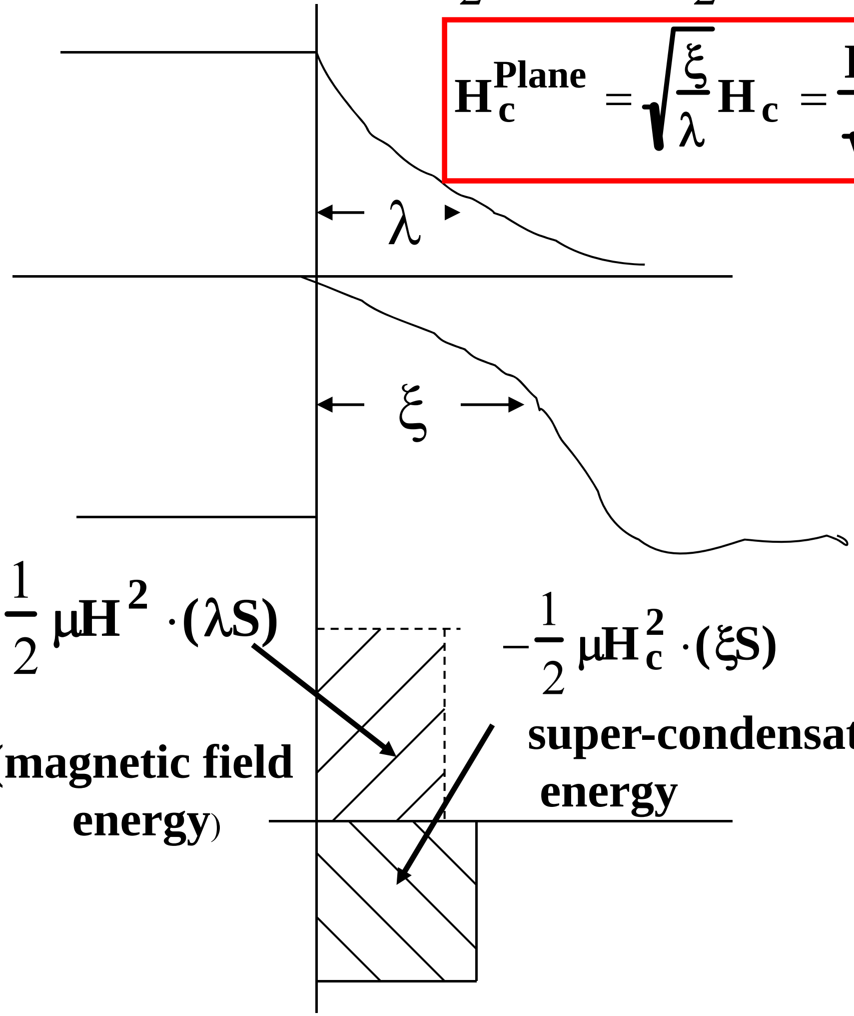

Vortex line nucleation

$$\frac{1}{2}\mu H^2 \lambda^2 - \frac{1}{2}\mu H_c^2 \xi^2 = 0$$

$$\boxed{H_c^{Line} = \frac{\xi}{\lambda} H_c = \frac{H_c}{\kappa}}$$

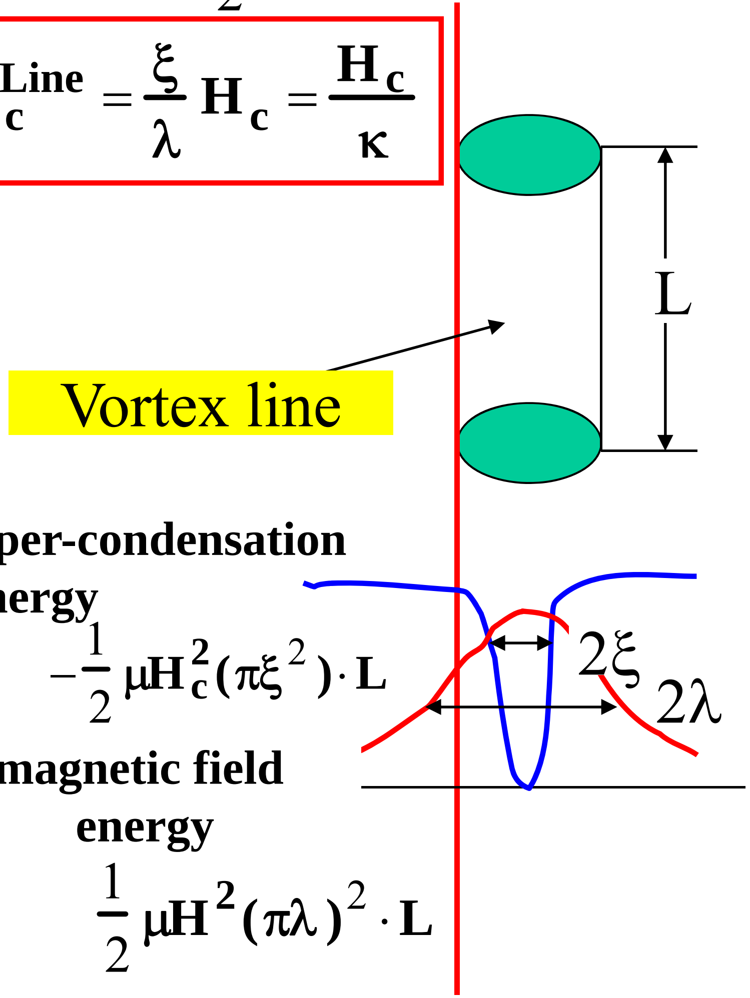

super-condensation energy

$$-\frac{1}{2}\mu H_c^2 (\pi \xi^2) \cdot L$$

magnetic field energy

$$\frac{1}{2}\mu H^2 (\pi \lambda)^2 \cdot L$$

RF Field limitation of vortex line nucleation

$$\frac{1}{2}\mu H^2\lambda^2 - \frac{1}{2}\mu H_c^2\xi^2 = 0$$

$$H_c^{Line} = \frac{\xi}{\lambda} H_c = \frac{H_c}{\kappa}$$

Effective field strength

$$H_c^{Line}(T) = \frac{\xi(T)}{\lambda(T)} \cdot \sqrt{2} H_c(T) = \frac{\sqrt{2} H_c(T)}{\kappa(T)} = \sqrt{2}\frac{H_c(0)}{\kappa(0)} \cdot \left[1 - \left(\frac{T}{T_c}\right)^4\right]$$

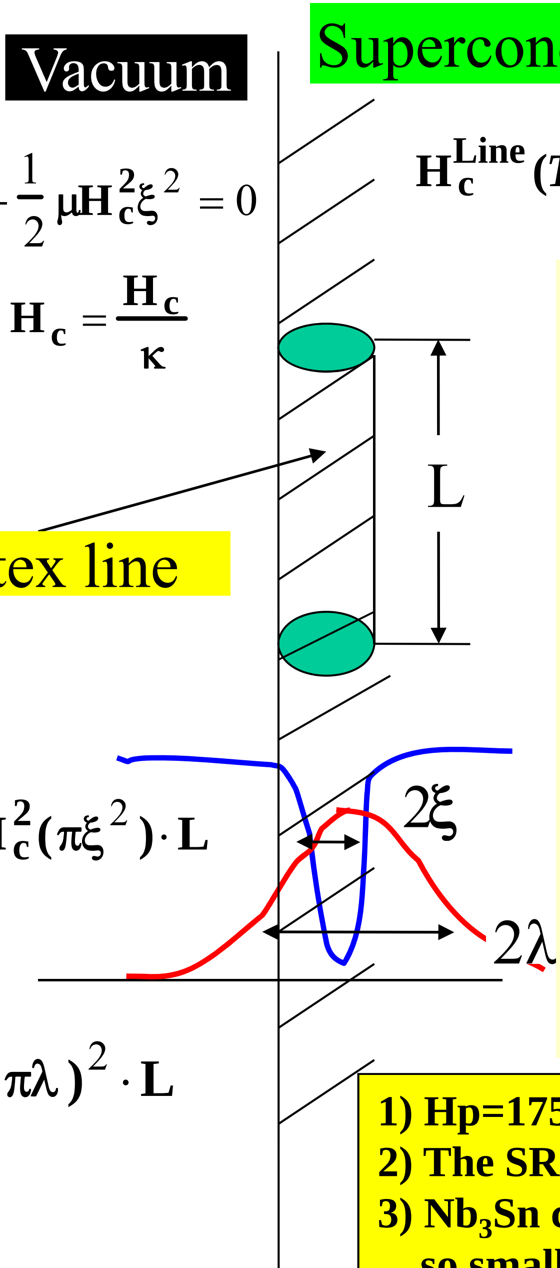

$$-\frac{1}{2}\mu H_c^2(\pi\xi^2)\cdot L$$

$$\frac{1}{2}\mu H^2(\pi\lambda)^2\cdot L$$

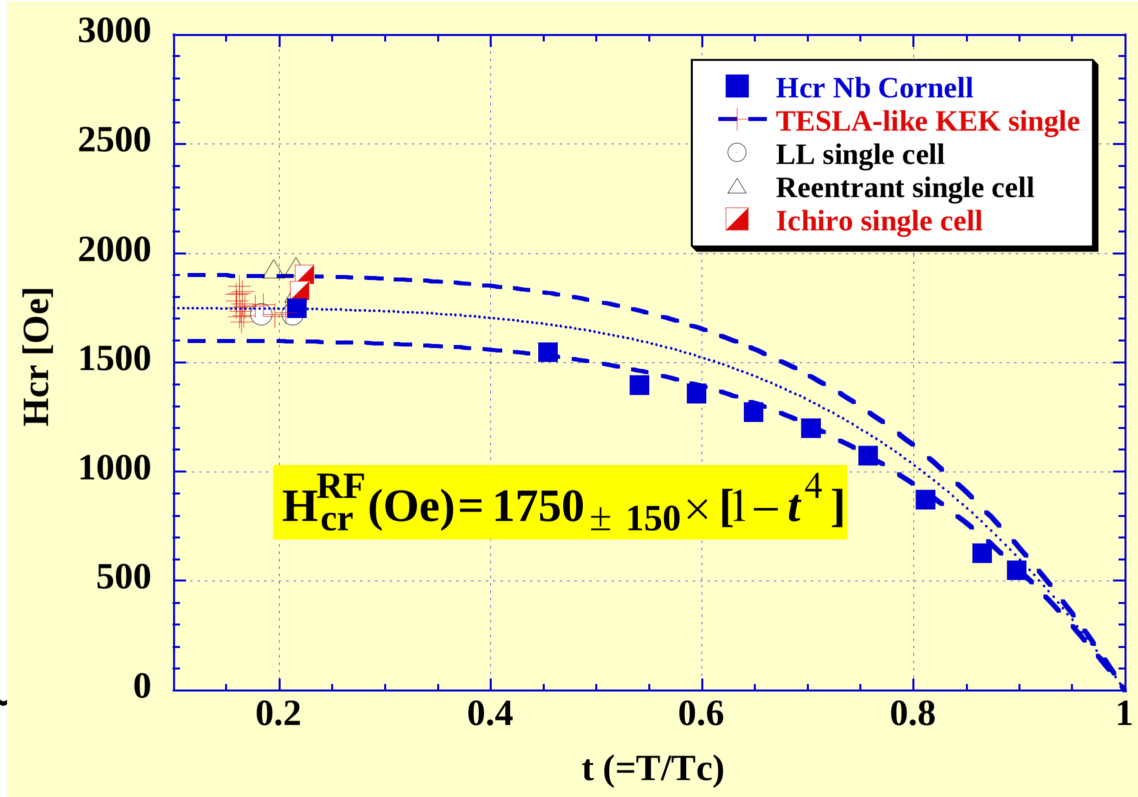

1) Hp=1750±50 Oe with Nb cavity ⟶ Eacc ~ 40MV/m
2) The SRF technology is meeting the theoretical limit.
3) Nb_3Sn cavity has a very larger k(0), therefore the critical field is so small.

他の材料(Nb_3S_n, Pb)の空洞に対する有効性のチェック

第2種超伝導体については非常に有効！

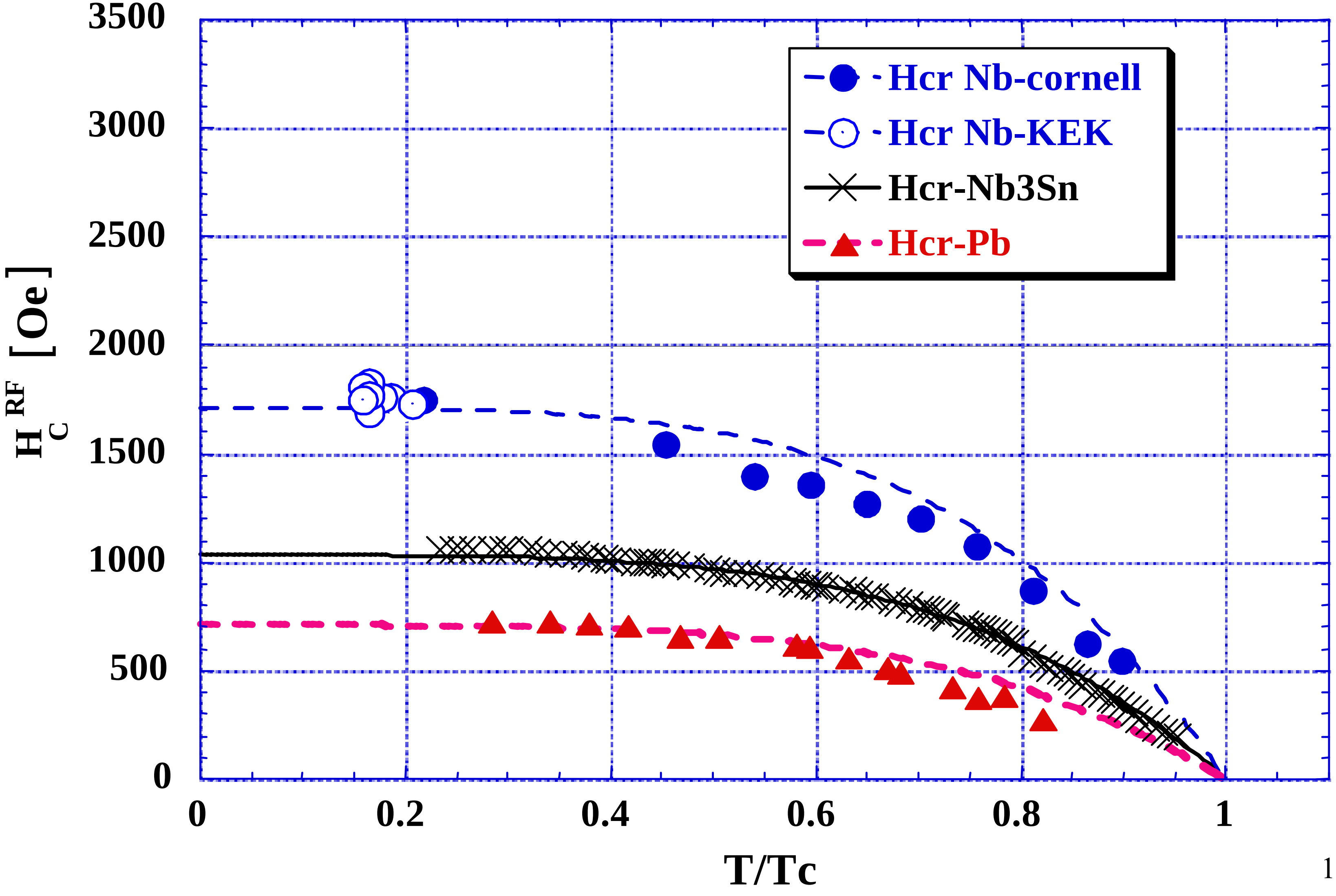

What material is best ?

Material point of view:

- Smaller heat loading for refrigerator ➡ Higher T_C
- High gradient

  $H_{RF} > H_C^{RF}$, then normal conducting

$$H_c^{RF} = \sqrt{2} \cdot \frac{H_c}{\kappa}, \ \kappa : \text{G - L parameter}$$

  The material with higher Hc and smaller κ-value

If Hc is high enough, Type-I material is better because of the smaller κ-value.

- Good formability

Materials	Tc [K]	Hc, Hc1 [Gauss]	Type	Fabrication
Pb	7.2	803	I	Electroplating
Nb	9.25	1900, 1700	II	Deep drawing, film
Nb_3Sn	18.2	5350, 300	II	Film
MgB_2	39	4290, 300	II	Film

Niobium has higher Tc, Hc and enough formability.

Now, niobium is widely used for RF sc cavity production.

2. Summary

1) 超伝導体の**AC/RF**応用では、**DC**応用と異なり表面抵抗が発生する。
その値は非常に小さいが、液体ヘリウムの負荷としては無視出来ない。

2) SRF応用では**Tc**、**Hc**が高く、**κ**の小さい材料が良い。また、成型性が要求される。

3) ニオブは、これらのパラメターを全体的に満たす材料であり、広く使われている。

4) 工業的に生産されるニオブ材は**RRR>100**であれば、実験室レベルの性質を備えており、第２種超伝導材料の理論が適用できる。

5) 空洞製作に際しては、表面欠陥によるクエンチが起こるので、極低温でも高熱伝導率が要求される。熱伝導率は**RRR**に比例し、測定が簡単なので、ニオブ材の良し悪しはもっぱら**RRR**の値で評価される。